Mechanisms of earthquake induced chemical and fluid transport to carbonate groundwater springs after earthquakes

Michael R. Rosen[1,2], Gilberto Binda[3], Claire Archer[4], Andrea Pozzi[3], Alessandro M. Michetti[3], Paula J. Noble[4,2]

[1]*United States Geological Survey; Carson City, NV, USA*

[2]*Global Water Center; University of Nevada, Reno, NV, USA*

[3]*Dipartimento di Scienza e Alta Tecnologia, Università degli Studi dell'Insubria, Via Valleggio 11, Como, Italy*

[4]*Department of Geological Sciences and Engineering; University of Nevada, Reno, NV, USA*

This article has been accepted for publication and undergone full peer review but has not been through the copyediting, typesetting, pagination and proofreading process which may lead to differences between this version and the Version of Record. Please cite this article as an 'Accepted Article', doi: 10.1029/2017WR022097

Abstract

Mechanisms by which hydrochemical changes occur after earthquakes are not well documented. We use the 2016-2017 central Italy seismic sequence, which caused notable hydrochemical transient variations in groundwater springs to address this topic, with special reference to effects on fractured carbonate aquifers. Hydrochemistry measured before and after the earthquakes at four springs at varying distances from the epicenters all showed immediate post-mainshock peaks in trace element concentrations, but little change in major elements. Most parameters returned to pre-earthquake values before the last events of the seismic sequence. The source of solutes, particularly trace elements, is longer residence time pore water stored in slow moving fractures or abandoned karstic flowpaths. These fluids were expelled into the main flow paths after an increase in pore pressure, hydraulic conductivity, and shaking from co-seismic aquifer stress. The weak response to the later earthquakes is explained by progressive depletion of high solute fluids as earlier shocks flushed out the stored fluids in the fractures. Spring $\delta^{13}C_{DIC}$ values closest to a deep magma source to the west became enriched relative to pre-earthquake values following the August 24th event. This enrichment indicates input from deeply-sourced dissolved CO_2 gas after dilation of specific fault conduits. Differences in carbon isotopic responses between springs are attributed to proximity to the deep CO_2 source. Most of the transient chemical changes seen in the three fractured carbonate aquifers are attributed to local shaking and emptying of isolated pores and fractures, and are not from rapid upward movement of deep fluids.

Keywords: Central Italy, 2016-2017 Earthquakes, Fractured Carbonate Aquifers, Water Quality, Carbonate Groundwater Springs, Temporal Change.

Key Points

- Transient changes in trace elements after earthquakes in fractured carbonate aquifers are due to local ground shaking not deep fluid movement
- Changes in carbon isotopic ratio in some springs near a deep magma source indicate release of dissolved CO_2 gas after shaking
- Shaking out long residence time water from isolated pores and fractures into the main flowpath is the reason for the transient response

1. Introduction

Co-seismic hydrological and chemical response at groundwater springs following strong earthquakes is a significant concern worldwide, especially where groundwater is an important resource (Barberio et al., 2017; Pasvanoglu et al., 2004; Reddy et al., 2011; Skelton et al., 2008; Skelton et al., 2014).

The pre-, co- and post-seismic changes observable in groundwater can be attributed to several factors originating from: 1) strain and/or rupture along faults or fractures changing the properties of the aquifer containing that groundwater (Reddy et al. 2011, Woith et al. 2013), 2) dilation of surface rock from shaking that promotes release of locally stagnant fluids (Pasvanoglu et al, 2004; Charmoille et al., 2005), 3) dilation and mixing of different aquifer water (Skelton et al., 2014), 4) deep-seated geothermal fluids released during dilation of rocks at depth (Barberio et al., 2017), or 5) release of deep-seated gases through dilation or fault rupture caused by over-pressurization in geologic traps (Chiodini et al., 2004). These possible mechanisms can occur in any rock type, but only some water quality changes have been well-documented in fractured carbonate

aquifers (Table 1). Some of the mechanisms documenting change in flow or water quality after earthquakes may be long-term, generally the ones that change the structure or placement of the water in the aquifer such as those related to fault movement. Most, however, appear to cause temporary changes to water quality and flow due to the transient nature of the mechanism, such as dilation or release of over-pressured gases and fluids that return to pre-earthquake conditions after the shaking has stopped.

The strain or stress provided by an earthquake can be divided into static and dynamic components: the former due to the movement or fault offset and the latter due to the strain from seismic waves on the aquifer (Manga & Wang, 2015). Groundwater response at varying distances from the epicenter has been widely documented in various rock types (Barberio et al., 2017; Claesson et al., 2004; Hartmann & Levy, 2006; Falcone et al., 2012, La Vigna et al., 2012; Skelton et al., 2014) as changes in groundwater level, spring discharge, or groundwater physical and chemical parameters. The distance from epicenter to groundwater, termed near-field (within the distance of the ruptured fault length), intermediate field (1-10 ruptured fault lengths) and far-field (greater than 10 ruptured fault lengths) by previous studies (La Vigna et al., 2012; Wang & Manga, 2010), is important as dynamic and static stresses caused by the earthquake decay differently with distance, and categorization may help predict earthquake hydrologic effects. The response, duration, and propagation distance of changes in water quality and groundwater flow depends on the aquifer hydrogeology, pore pressure spread, and the earthquake strength (Ingebristen & Manga, 2014; Manga & Wang, 2015). It is also important to consider the temporal component by determining the short- mid- and long-term effects on regional groundwater systems, particularly because permanent deformation of large aquifers can impact major drinking water sources (Malakootian & Nouri, 2010). In

fractured carbonate aquifers like those in the Apennines, transient responses are common as new microfractures are formed, existing fractures are cleared, and new flow paths form but eventually return to their original state (Amoruso et al., 2011; Galassi et al., 2014).

The Apennines, a mountain belt in central Italy characterized by regional carbonate groundwater systems interacting with active normal faults capable of producing Mw 6.5 to 7.0 seismic events (e.g., Cello et al., 1997; Roberts & Michetti, 2004), are particularly susceptible to alteration due to earthquakes. These aquifers also provide water supply to major metropolitan areas in the region. The observations made during the 2016-2017 seismic sequence in Central Italy provide a valuable dataset for analyzing major mechanisms of earthquake induced chemical and fluid transport to fractured carbonate aquifer springs after earthquakes. We argue that this is relevant for better understanding the relations among tectonic deformation affecting large aquifers, strong release of seismic energy and hydrochemical parameters.

On 24 August 2016, the first main shock (Mw= 6.0) of the 2016-17 central Italy Seismic Sequence (also known as the 2016 Amatrice-Norcia seismic sequence; e.g., Chiaraluce et al., 2017) struck the central Apennines in the area where Latium joins Umbria, Marche and Abruzzi and was followed one hour later by a Mw 5.4 shock. The epicenter of the event was located at the segment boundary between the Mt. Vettore and Mt. Laga faults (Figure 1), and ca. 7 km of coseismic surface faulting was mapped near Monte Vettoretto (Livio et al., 2016). On 26 October 2016 and on 30 October 2016, three other big shocks (Mw 5.5, Mw 5.9 and Mw 6.5, respectively) ruptured again the Vettore Fault and its NW extension, with a total surface faulting length of ca. 30 km (Civico et al., 2017). On 18 January 2017, four shocks with magnitude greater than 5.0 struck the Campotosto Fault, a different segment to the SE extension of the previous events, with a

mainshock of Mw 5.7. The seismic sequence totaled over 26,000 earthquakes, including aftershocks, activating two major fault segments and spanning over 40 km (Chiaraluce et al., 2017). The 30 October 2016 shock was the largest event to hit the central - southern Apennines in 26 years (Chiaraluce et al., 2017).

Barberio et al. (2017) sampled a 100 m deep well and springs in the Sulmona Plain Test Site (SPTS), which is located approximate 70 km southeast of the central area of the earthquake activity during 2016-2017. They measured major and trace element concentrations before and after the seismic sequence and found transient changes in concentrations of some trace elements that they attributed to release of geothermal fluids and/or deeply-trapped CO_2 from the deep subsurface through dilation, fluid-rock interaction, and fluid ascent.

This study reports on the groundwater hydrochemical response to the seismic sequence of August 2016 - January 2017 from two high flow carbonate springs and one alluvial spring located in the Rieti area (Latium region), within the intermediate field, 30-40 km away from all the epicentral areas, and in one instance a carbonate sourced spring in the Nerea area within 5 km of the epicentral area (near-field) for the October shocks, the Uccelletto spring in Castelsantagelo sul Nera, (Marche region). The Rieti area springs benefit from the availability of pre-seismic data from 2014-2015 collected by Archer et al (2016). The presence of a water bottling plant at Uccelletto spring allowed us to sample archived water collected monthly for 10 months before the earthquakes at Nerea, as well as co- and post seismic sampling conducted as part of this study (see supplementary data ds01a-d for all the data used in this study).

Similar to Barbiero et al. (2017), we report the hydrochemical responses to the 2016-2017 central Italy seismic sequence, but rather than highlighting the reported

potential of seismic precursor signals, we focus on a comparison of responses in the near and intermediate-field areas with the goal of better conceptualizing the mechanisms and documenting the spatio-temporal variability of these responses highlighted in Table 1 in carbonate aquifers. The aquifers studied here were subjected to the direct effects of shaking and tectonic displacement of large hydrogeologic structures, which in turn affected the flow paths, hydrochemistry of the groundwater, and flow dynamics on different time scales.

2. Study Area

2.1. Tectonic Setting

Major aquifers in the central Apennines are hosted within fractured Meso-Cenozoic carbonate massifs that overly an evaporitic basal structure (Quattrocchi, 1999). Recharge occurs mainly at high-elevation and aquifers are characterized by two major flowpaths: one shallower with high flow rates through major discontinuities and the other with low to medium flow rates where seepage or uprising of deep mineralized fluids occurs along fractures (Amoruso et al. 2011, Petitta et al. 2011). This dual- or multiple-flow structure allows for differences in residence time of waters within the same aquifer. The major faults and tectonic structure of these aquifers can serve two purposes: allowing the upwelling of deep mineralized fluids and mixing of groundwater with different chemistries (Barberio et al., 2017; Petitta et al. 2011), or compartmentalizing the aquifer, acting as lower permeability aquicludes (Amoruso et al. 2011). The mineralized waters containing dissolved CO_2 sourced from the mantle are found in a reservoir within the Mesozoic basement rock unit that, based on ^{13}C isotopic evidence, is originally sourced from deeper within the crust or mantle (Chiodini et al. 2004, Petitta et al. 2011). The low-

permeability portion of these aquifers contains water with higher concentrations of dissolved ions, including trace elements (Morgantini et al. 2009).

The ruptured faults from the Amatrice-Norcia seismic sequence are located within a relay zone between two major overlapping NNW–SSE trending normal faults in the Central Apennines. The Apennines fold-thrust belt is part of the accretionary wedge caused by the roll back of the Adriatic subduction towards the east (Cavinato & De Celles, 1999). The Plio-Quaternary normal faults, formed by the subsequent west-to-east migration of the regional extensional regime, govern the intra-montane basin evolution and its filling through continental clastic deposits and also are capable of producing large devastating earthquakes (Mw 6 to 7; e.g., Roberts & Michetti, 2004). The ruptured fault segments are focused on either side of the Olevano–Antrodoco–Sibillini (OAS) thrust system, and surface faulting occurred in between two similar surface rupturing seismic sequences that occurred in the central Apennine in the past 20 years: the 1997 Colfiorito sequence to the north, and the 2009 L'Aquila events to the south (Vittori et al., 2000, 2011)

2.2. Hydrogeological Setting

2.2.1.Nerea Area

The Nerea spring (NER) recharge area (Figure 1) is a major fractured carbonate aquifer within the Umbria-Marche carbonate ridge that is characteristic of the central Apennines (Mastrorillo and Petitta, 2014). In these karstic large-area aquifers, faults and fractures within the limestone control flow (Amoruso et al., 2011). The aqueduct feeding the Nerea S.p.A bottling plant was sampled during this study from archived water samples that were stored as part of the bottling plant commercial license. The aqueduct

flows from the Uccelletto spring, with a discharge measured at 0.57 m^3/s sourced from the Nera-Ussita basal aquifer (Tarragoni, 2006). Pre, co- and post-seismic chemical data were made available from the Uccelletto spring in Castelsantagelo sul Nera through access to the Nerea S.p.A. bottling plant's archived quality control samples. Dates of monthly pre-earthquake samples analyzed (10 samples) for this study begin in November 2015 and end in August 2016 (two weeks before the first earthquake). See supplementary data ds01 for more details.

2.2.2. Rieti Area

Deep normal faults at the border of the Rieti plain separate the marine Meso-Cenozoic carbonate ridges from Plio-Quaternary continental deposits. This structural style is characteristic of central Apennine extensional-basins, where the regional flow system is hosted by the surrounding carbonate bedrock and many springs discharge at the contacts with lower-permeability basin deposits (Martarelli et al., 2008). In general, the hydrogeological unit (Catena Nuria-Velino-Monte Giano) has an area of about 1200 km^2 and the thickness of the carbonate aquifer can reach 3000 – 4000 m (Celico, 1983; Boni et al., 1988; Civita & Fiorucci, 2010). At the northeastern edge of the Rieti Plain, Santa Susanna Spring (SUS), the highest discharge spring (5.5 m^3/s) of those in direct contact with the plain, is supplied by base-flow of the regional aquifer, and emerges at the intersection of two normal faults (Guerrieri et al., 2006). This regional aquifer is hosted in the Terminillo and Reatini mountain carbonates to the east with infiltration of 545 mm/yr and total recharge area over 300 km^2 (Spadoni et al., 2010). The aquifer host rock consists of imbricate thrust carbonates with evaporitic gypsum and anhydrite units in the subsurface (Martarelli et al., 2008; Spadoni et al., 2010). The aquifer geology is reflected

in the SUS water chemistry, which has the highest EC and the highest sulfate concentration of all the springs sampled in this study (Archer et al., 2016). Locally, interbedded Triassic dolomitic limestone outcrops are present (Martarelli et al., 2008). The average residence time of water in this aquifer is on the order of 15-20 years, calculated using values of aquifer properties, recharge area and Euclidian distance to the spring (Spadoni et al., 2010).

Vicenna Riara Spring (VIC), located near the center of the Rieti Plain, is distinct among springs included in this study because it flows from a locally-recharged alluvial aquifer. Water flows to this spring along a buried fault and through preferential flow-paths within the Pleistocene conglomeratic alluvium that lies in the central-eastern part of the plain. Compared to the discharge at SUS, VIC has a relatively low discharge of 0.07 m^3/s (Martarelli et al., 2008), but is the highest discharge alluvially-fed spring in the Rieti Plain.

Peschiera spring (PES) is located about 8 km to the east of the Rieti Plain in the Velino River Valley (Figure 1). PES has high discharge (i.e., 18 m^3/s) and represents a major drinking water supply to Rome.

The groundwater contribution to the spring is mainly from the aquifer hosted within the Triassic – Paleocene thrusted and uplifted evaporites and carbonate shelf deposits to the east-southeast located in the Giano-Nuria-Velino mountains (Civita & Fiorucci, 2010). In particular, the Triassic section of the aquifer includes dolostones, gypsum and anhydrite units (Pieri, 1966; Centamore et al., 2002; Barbieri et al., 2017). Though two flow paths have been identified to source the spring with significantly different mean residence times and amounts;10% of the water has a mean residence time

of ~25 – 30 years and 90% has a mean residence time of thousands of years (Civita & Fiorucci, 2010), we consider that only the faster circuit (~25 – 35 years mean residence time) in this aquifer, could be affected by the seismic sequence.

The recharge area for PES is delineated in Figure 1, and the mean infiltrating volume of water calculated by Civita and Fiorucci (2010) to be 17.87 m^3/s is essentially equal to discharge at the spring.

3. Methods

Water samples were collected in LPDE bottles and physiochemical parameters (pH, T, EC and alkalinity as HCO_3 by titration) were measured directly on site. Samples were then stabilized and stored refrigerated for laboratory analyses including:

- major ions (Na, Ca, Mg, K, Cl, SO_4) that were run through ionic chromatography;
- trace elements **(**Al, Cr, Mn, Co, Cu, Ni, Fe, Pb, U, Rb, Sr, Se, As, V, Li, B, and Cd) that were analyzed by Inductively Coupled Plasma -Mass Spectrometry (ICP-MS). The concentrations of As, Se, V, and Cd were equal to or lower than our limit of detection and these elements, as well as B and Li (which were detected) showed no discernable change throughout the sampling period. The limit of detection (LOD) for all trace element concentrations are listed in Appendix Table A1;
- $\delta^{34}S_{SO4}$ and $\delta^{18}O_{SO4}$ analysis using $BaSO_4$ precipitation,
- $\delta^{13}C_{DIC}$ by precipitation of $SrCO_3$,
- $\delta^{18}O_{H2O}$ using the CO_2 - H_2O equilibration method, and on-line chromium reduction using continuous-flow isotope ratio mass spectrometry for $\delta^{2}H_{H2O}$.

Data analysis was conducted using time series plots (with sample day as the shortest time interval of importance) to pick up any chemical anomalies that may have occurred during the earthquake sequence. In addition, a bivariate correlation matrix using Pearson correlation coefficients and a Principal Component Analysis (PCA) were applied to the dataset to ascertain whether there was a coherent seismic response among the correlated variables. Only the first two principal components were significant (>10 percent of the total variance). Chemical data were compared with meteorological (especially precipitation) and seismic data to check their relevance as drivers of observed chemical variations. B and Li were not included in the PCA because we had limited pre-earthquake data for these elements.

Bottled water samples used from Nerea Spa bottling plant were fed through a sand filter bed. It appears that the sand filter did not significantly impact the elemental data, as results collected from the spring and from the archived samples were similar, so the samples for both NER spring and the bottling plant will be interpreted together in this paper.

Detailed methodologies of the protocols, sample preparation, data reliability, and statistical techniques are included in appendix A1. All data can be found in Supporting Information ds01a-d.

4. Results

4.1. Flow

It was not possible to measure flow at the springs studied, either due to proprietary concerns of the spring owners or lack of appropriate measuring locations, and because of the lack of existing flow gauges at the sites. However, after the earthquake sequence an increase in water level in wells, as well as increase in flow in different springs were

observed by other researchers working contemporaneously in the area where this study was conducted (Checcucci et al., 2017; Barberio et al., 2017; Petitta et al., 2018) . The Nera River (which is sourced from NER spring) doubled in flow after the seismic sequence. In the upper part of the river, the flow increased from a baseline value of about 1.5 m^3/s to 3 m^3/s after the 30th October 2016 shock (Banzato et al., 2017). Moreover, a stream in the Norcia Basin (less than 10 km from the 30 October 2016 shock epicenter), which became dry after an earthquake in 1979, was re-activated just after the 30 October 2016 shock, and its flow increased in the following weeks (Valigi et al., 2017; Checcucci et al., 2017). Other springs and wells not sampled in this study around the Rieti Basin also increased in flow during the seismic sequence (Petitta et al, 2018).

4.2. Physico-Chemical Measurements

Electrical Conductivity values (Figure 2A) were elevated at SUS, VIC and PES after the August 24th mainshock, and then decreased over the next two-week period. Values at all four springs were elevated at the onset of sampling after 24 August, into October. After the 30 October mainshock, SUS and PES increased again above the range of pre-earthquake values. NER exhibited an abrupt increase following the near field shocks of 26 October and 30 October and remained elevated until values decreased and returned to below pre-earthquake values by 18 November 2016. Alkalinity (Figure 2B) followed the same general pattern. The alkalinity at SUS and VIC returned to pre-earthquake values by 26 October, becoming elevated again in January 2017. PES alkalinity remained elevated until returning to pre-earthquake range by 17 May 2017. NER alkalinity increased sharply after the near –field shocks of 26 October and 30 October, peaking on 8 November 2016. Both EC and alkalinity showed only minor variability after the 18 January 2017 earthquake.

The pH of SUS was slightly elevated after the earthquakes, but the increases didn't correspond to when the major earthquakes occurred (Supplementary Figure S1A). PES and VIC pH values were also higher than pre-earthquake values, but the increases were not correlated to earthquake occurrence (Supplementary Figure S1 B, C). NER pH didn't change compared to pre-earthquake values. The temperature measured at PES and SUS (Supporting Information ds01a) did not deviate outside the range of previous values during the post-earthquake time series. The exception was one measurement of PES on 30 August was abnormally high at 15.9°C. The temperature of VIC in all measurements during the post-earthquake time series was 0.4 – 1.0°C higher than the pre-earthquake range.

4.3. Major and Minor Ions

The springs are dominated by Ca and HCO_3 due to the dominant calcium carbonate rock type (Supplementary Figure S2). Where gypsum is present in the aquifer at SUS, the composition of the water is Ca-SO_4-HCO_3. Where dolomite is present, Mg has higher concentrations in the water (SUS, PES). Although VIC is an alluvial spring, the dominant rock type is limestone and so has a similar major ion composition to the other springs. Major ions increased slightly after the earthquakes, although each spring responded differently. NER major ions did not change over the earthquake sequence. In the Rieti Basin springs, Mg and K increased in all springs, but Na only increased at SUS and VIC. These changes were not large, less than 25% of pre-earthquake values. Minor ions (NH_4, NO_2, NO_3, F and PO_4) showed no changes throughout the pre-, co- and post-seismic time periods, and F, PO_4 and NO_2 were below the LOD in most of the samples analyzed (Supporting Information ds01a). Concentrations of Cl did not change

significantly at any of the springs measured. Concentrations of SO_4 showed no change at NER, but at VIC, PES and SUS there was an abrupt increase after the August earthquake and another increase after the 30 October 2016 earthquake at VIC only (Figure 2C). This was followed by a decrease until reaching pre-earthquake concentrations in ca. 3 months, a trend that mirrors the trace element response (see below).

4.4. Trace Elements

Figure 3A-F shows concentrations of representative trace elements (Al, Cu, Pb, Sr, Rb, Mn) in time series for all sampled springs. Other trace elements (Cr, Co, U, Fe, Ni) not displayed in Figure 3 also demonstrate similar trends. A significant number of trace elements (Al, Cu, Pb, Sr, Rb, Mn, Cr, Co, U, Fe, Ni) in the three Rieti area springs show elevated concentrations following the August. 24th earthquake when compared to pre-earthquake values measured from the September 2015 samples (Figure 3). Two exceptions to this pattern are Rb in SUS and Sr in VIC. The concentrations of Al, Mn, Pb, Co, Fe and Ni in the Rieti springs are strongly correlated, with Pearson correlation coefficients >0.9 (Supporting Information ds01c). The trace elements at PES show two main peaks in concentration concurrent with the August and October mainshocks, with a smaller peak above pre-earthquake values at the January mainshock. At SUS, the peak concentrations occurred after the August. 24th mainshock, then concentrations gradually decreased over the sampling period. Rb and U are highly correlated at all springs and exhibit a slight peak in concentration following the August. 24th mainshock (Rieti springs), with a gradual decrease over the rest of the time series. PES values of these elements peaked during the August sampling then again at the Oct 31st sampling. Sr concentrations were high after the August. 24th event, did not show major change after

the October 24th and 30th events, but then increased again at the end of the sampling (February, April 2017) in PES and SUS. The Sr concentration at NER did not show significant variability. NER Al, Cu, Mn, Pb and Ni concentrations also exhibited minor peaks after the October 24th and 30th earthquakes and during mid-November as well as mid-January, prior to the January 18th mainshock.

Pearson correlation tests performed for each spring show strong correlations (>0.5) between the concentrations of many element pairs. Precipitation is moderately to weakly correlated (<0.5) with all element concentrations in all springs, except for Fe in PES, which is negatively correlated (-0.775). Correlation matrices can be found in Supporting Information ds01c.

The coherent response in elemental chemistry is also illustrated in the results of the PCA. The trace element and major ion concentration data show high negative loading values for Component 1, associated with the large suite of trace elements, including Mn, Fe, Ni, Pb, Al, Cu and Cr, and some major elements, and explains ~42% of the total variance (Figure 4A). Similar to the individual time series plots of metals (Figures 3A-F), the first component score values plotted in time series, for NER spring and bottle samples (Figure 4B) show a strong increase in concentration and score values after the 26 and 30 October shocks then are unstable for ~two months until January 2017 when values become similar to the pre-earthquake values.

A time series plot of Component 1 scores of the Rieti area springs shows that the strong release of metals occurred mainly after the August 24th shock, with some variation in the recovery between the three springs (Figure 4B). Similar to the NER samples, the scores return to baseline values that are near those observed prior to the earthquake.

Moreover, Rieti springs show score values larger than NER. This is due to higher constituent concentrations for the metals in Rieti springs, compared to NER.

The PCA also shows that ~20% of the total variance can be explained by Component 2 (Figure 4A). This variance divides the elements into 2 groups; Sr, SO_4, Mg, Ca, U, Rb with negative loadings, and Fe, Cu, Al, Pb, Na, K, NO_3, Cl, and Co with positive loadings. Alkalinity (HCO_3) has a loading that is near zero, and is between the two groups. Overall, NER samples don't show much variability in Component 2 scores, so this response is reflective of the Rieti area springs only. When Component 2 is plotted in time series for the Rieti samples (Figure 4C) there are lower score values following the August 24th event, reflective of increased concentrations of Sr, U, Rb, Ca, Mg, and SO_4.

Ammonia and pH show little variation and do not show any correlation with other major or trace elements (Figure 4A).

4.5. Stable Isotopes

The $\delta^{13}C_{DIC}$ values (Figure 5A) of SUS became 1-2‰ enriched above pre-earthquake samples during the August and September samplings. The October 31st and November 10th samples then show enrichments up to 6‰ greater than before the earthquakes. Values of $\delta^{13}C_{DIC}$ for PES also show enrichment above the range of previous values following the August 24th earthquake, then remain enriched during the post-seismic time series. The most enriched value of $\delta^{13}C_{DIC}$ at PES occurred on October 31st. Values at VIC were slightly heavier than pre-earthquake values and enriched in the November sampling dates following the October mainshocks. The three pre-earthquake samples at NER were all from 2016, with $\delta^{13}C_{DIC}$ values between -10 and -12‰. The post-earthquake sample values are also within this range except for those within a few days

following the October mainshocks, where $\delta^{13}C_{DIC}$ values became up to 5‰ more negative.

The $\delta^{18}O_{SO4}$ of SUS show no discernible response to seismicity (Figure 5B), but for PES the value of $\delta^{18}O_{SO4}$ was significantly enriched for two samples after the first mainshock (August 27th, 28th). Values of $\delta^{18}O_{SO4}$ of VIC also show enrichment in two samples; August 28th and August 30th, while $\delta^{34}S_{SO4}$ do not vary outside of the pre-earthquake range (Supporting Information ds01b). The co- and post-seismic $\delta^{34}S_{SO4}$ of all three localities was within the variability of our measured pre-seismic values. Due to the relatively low volume of archived water available, and the low amount of total sulfate in the water, $\delta^{34}S_{SO4}$ and $\delta^{18}O_{SO4}$ were not analyzed for NER springs.

Values of $\delta^{18}O_{H2O}$ and $\delta^{2}H_{H2O}$ are plotted with the global meteoric water line, Mediterranean meteoric water line, and the central Italian meteoric water line (Giustini et al., 2016) in Figure 6. The values of VIC, SUS, PES and NER did not change significantly post-earthquake as compared to pre-earthquake value ranges. The pre-earthquake values were collected in all seasons and do not exhibit significant seasonal variability during the years sampled. However, the isotopic values demonstrate that recharge elevations for the springs vary from relatively low elevation at VIC, to recharge elevations >1400 m for NER springs (Figure 6).

5. Discussion

5.1. Natural Variability

To assess whether seismic shaking or changes in pressure, fluid flow, or release of new sources of water to the aquifer caused the changes in groundwater chemistry observed after the earthquake sequence, yearly seasonal changes in groundwater

chemistry caused by winter recharge must be ruled out. Previous work on the recharge and discharge processes of SUS and PES springs estimated aquifer mean residence times on the order of 15 – 35 years.

These calculations, however, do not reflect the dual-flow nature of these aquifers, where basal spring discharge contains a mixture of water from the fast (on the order of days), and slow (on the order of years to tens of years) flow paths (Amoruso et al. 2011; Petitta et al. 2011; Nanni & Rusi, 2003). The precipitation patterns characterizing this region predict that the majority of aquifer recharge occurs in the wetter winter months. The Apennine snow pack is between 1 and 3.5 m, on average, and the mantle of snow generally persists no more than 100 days, apart from at the highest peaks (Costantini et al. 2013).

To test that the seasonal recharge from snow melt was not influencing the observed hydrochemical trends in these springs, the fastest possible recharge to discharge flow path (i.e. days) was considered in testing for trace element concentration correlation with each other and with precipitation amounts during the month prior to sampling (Supporting Information ds01d). The amount of precipitation between samplings does not correlate with measured trace element concentrations, indicating that water recharging between an earthquake event and water sampling at the spring did not influence these measurements. The Fe concentration in PES is negatively correlated with precipitation and could indicate a change in redox conditions due to oxygenated snow melt that caused reduced iron to drop out of solution. However, this is unlikely because this is the only spring and element where this association exists and other redox sensitive elements (Mn, Cr, As, Se) did not react the same way.

5.2. Differences in Response between Springs

5.2.1. Major Elements

Most major element concentrations did not increase significantly during the earthquake sequence, but some constituents such as Mg, K., SO_4, and HCO_3 (alkalinity) increased in the Rieti area springs (SUS and PES), particularly after the 24 August 2016 earthquake (Figure 2B). The pre- and post-earthquake values of stable isotopes of water show no change for any of the springs (Figure 6) and indicate a lack of mixing of different source of waters, unless the waters mixed shared the same recharge elevation. Additionally, the lack of substantial change in the major element chemistry indicates that if mixing with a different source of water occurred, that the new source of water had either a small volume or a similar composition to the aquifer water. The exception to this is the concentration of SO_4 at SUS and PES (Figure 2C). The SO_4 concentration at these springs almost doubled after the August earthquake. The high concentration of SO_4 likely reflects the addition of slow moving water derived from contact with gypsum, which is prevalent in the Triassic rocks that contribute to these springs (Pieri, 1966; Centamore et al., 2002). Gypsum is not dominant in the aquifer that feeds the NER spring (note the low concentrations of SO_4 in the spring), and geologic cross sections indicate evaporitic beds are only found at considerable depth (Fusari et al., 2017; Pizzi et al., 2017). Gypsum bearing strata or waters that encounter such strata may have some input to VIC because the SO_4 concentration rose after the August earthquake. However, in the case of VIC, pre-earthquake variability approaches that of the post-earthquake response (Figure 3) so may not uniquely be tied to seismicity.

Alkalinity also rose slightly after the August earthquake at VIC, and PES and stayed high at PES until sampling stopped. At NER alkalinity rose only after the October

earthquakes. The likely reason for the NER response being confined to the October earthquakes is that NER shows a weak intermediate-field response to the August event, but a strong near-field response to the October events.

The lack of substantial change in the major ion chemistry of the springs after the earthquakes points to a small volume of water infiltrating the springs from pore spaces that were unconnected to the flow before the earthquakes. The addition of major ions from the closed pore spaces is proportionately small relative to the concentrations already present in the short travel time part of the aquifer, and are not going to result in a noticeable increase. The major ions in the pore spaces are expected to be similar in composition to those throughout short travel time part of the aquifer. In contrast, trace element concentrations, particularly for those elements that present very low concentrations (near or below detection limits) in the short travel time part of the aquifer, will transiently increase with the addition from a small volume of high concentration pore water.

5.2.2. Trace Elements

In general, all three Rieti springs show the greatest change in trace element composition after the 24 August 2016 earthquake and most trace elements remained elevated until after the October 26th and 30th, 2016 earthquakes. Most trace elements returned to background concentrations by the end of November 2016, and were not greatly affected by the January 18, 2017 earthquake, except Mn concentrations that appear to increase after each earthquake in VIC. The trace element response at NER appears to be delayed and most trace elements increased near October 1st, 2016, more than a month after the August earthquake, but become even more elevated after the October 26th and 30th earthquakes. Trace element concentrations at NER return to pre-

earthquake concentrations by the end of November, similar to the Rieti Springs (Figure 3).

The concentrations of Rb, Sr, and U did not show the same progressive decrease over the time series as the other elements, but remained elevated above 2015 values for the entire sampling. Rb, Sr and U are likely to substitute for Ca or Mg in the calcite or dolomite crystal lattice and so are likely associated with the carbonate rocks that dominate these aquifers. The other trace elements, in contrast, are more likely associated with clays and organic colloids in the slow-moving fractures and pore spaces. This is highlighted in the PCA analyses as Rb, Sr, U, SO_4, Mg and Ca all group in same quadrant of the diagram while all other trace and major elements plot in a different quadrant (Figure 5a), likely associated with clay minerals.

Variability in response among measured trace elements and springs could also be due to the properties of the elements such as redox potential or sorption (Drever, 2005) or their abundance in the different aquifers. For instance, Al concentration is affected by the distribution of clays in aquifers (Morgantini et al., 2009), so the high concentrations of Al in VIC, where recharge and discharge occur in a thick alluvial unit (Martarelli et al., 2008), can be attributed to more available clays within the pore matrix that can be released from co-seismic shaking. Increase of Fe and Mn concentrations in VIC may be related to release of more reduced water trapped in isolated pores and fractures.

The difference in response between the NER and Rieti springs may be related to their location in relation to the major earthquake epicenters (Figure 1). As mentioned above, the October earthquakes were centered much closer to NER than either the August or January earthquakes and so the response for the August earthquake (which was closer to Rieti springs) may have been delayed at NER. The lack of response to the January 18,

2017 earthquake at all springs sampled, may be because it was the furthest away from all the springs sampled (Figure 1), more than 20 km for all sites.

The proposed mechanism for the greatest change in trace element concentration occurring after the first earthquake and diminishing after the October earthquakes, is that the first event effectively cleared, or flushed out, the pore spaces or fractures where longer mean residence time groundwater collected (Figure 7; Galassi et al., 2014 Pasvanoglu et al., 2004), and none or less longer-residence time water was available for release after subsequent earthquakes.

The transient increase in trace elements in the aquifer, has implications for providing water to earthquake survivors immediately after earthquakes. Although the trace element concentrations in this study are not above drinking water standards, in places where background concentrations are higher, water supplies could be significantly affected for months after a strong earthquake.

5.2.3. Stable Isotopes

The values of $\delta^{18}O_{H2O}$ and $\delta^{2}H_{H2O}$ in Central Apennine groundwater are primarily controlled by recharge elevation (Longinelli and Selmo 2003; Petitta et al., 2011;). Hydrochemical responses have been observed in different settings that include post-seismic changes in $\delta^{18}O_{H2O}$ and $\delta^{2}H_{H2O}$ groundwater values. These changes have been attributed to aquifer breaching causing a change in aquifer structure or mixing of different groundwater components (Barbieri et al., 2005; Claesson et al., 2004; Reddy et al., 2011; Skelton et al., 2014).

The lack of a change in water isotope values of PES, SUS and VIC post-earthquake (Figure 6) supports the assumption that increases observed in groundwater chemical constituents are a result of processes occurring within the aquifer instead of

addition of water from another aquifer or from a geothermally heated source, which would have a different isotopic composition. The residence time in these aquifers is sufficiently long so that aquifer flowpath changes would not be evident in the $\delta^{18}O_{H2O}$ and $\delta^{2}H_{H2O}$ values until several years after the seismic sequence, if at all, especially because both SUS and PES are basal springs and represent an integration of flow within the aquifers (Civita & Fiorucci, 2010; Spadoni et al., 2010). This intra-annual stability is also displayed by the lack of variation in $\delta^{18}O_{H2O}$ and $\delta^{2}H_{H2O}$ during the pre-earthquake sampling period (2014-2015, Figure 6).

The primary sources of dissolved inorganic carbon (DIC) in these aquifers is dissolution of carbonate rock along flow paths, organically-derived soil CO2 dissolved during infiltration (~-15 – -30‰), and/or CO2 dissolved in mineralized water with a deep-flow circuit and longer mean residence time (Chiodini et al., 2000; Petitta et al., 2011; Raco et al., 2013). The δ13C of the carbonate platform comprising Mt. Terminillo and the Reatini Mountains ranges from ~ +2‰ to +3‰, while in the north, near Nerea, carbonate δ13C range from ~+2‰ to +3.5‰ (Morettini et al., 2002). The contribution of carbonate dissolution to δ13CDIC in this region is +2.21‰ ± 0.66‰ (mean and standard deviation of 567 samples of Apennine carbonate rocks, referenced in Chiodini et al. (2004) and references therein). The range of δ13CDIC in central Apennine groundwater containing mantle-derived CO2 (Figure 1), calculated using a carbon mass-balance together with isotopic and hydrogeological data, is -5‰ to -1‰ (Chiodini et al., 2000, 2004). The post-mainshock δ13CDIC values measured in this study (-5‰ to -3‰, Figure 5a) fall within this range of groundwater that has a contribution of mantle-derived CO2. Alternatively, or together with the addition of deep-aquifer CO2 gas, an increased contribution of groundwater from longer residence time reservoirs, flow paths, or matrix

porosity with a greater degree of water-rock interaction and marine carbonate isotopic signature could have caused this shift to heavier δ13CDIC. The lack of a consistent post-seismic pH trend at NER, SUS, and VIC (Supporting Information ds01a, and Supporting Information Figure 1S) and the rapid onset of the carbon isotope enrichment in PES spring, but delayed enrichment at SUS spring (after the October earthquakes) suggest multiple drivers of the observed post-seismic δ13CDIC increase. As suggested by Chiodini et al. (2004), the high pore-pressure from mantle-derived CO2 gas in these deep reservoirs may have instigated the fault rupture of these earthquakes and released CO2.

The $\delta^{13}C_{DIC}$ at VIC, however, did not change significantly from pre-earthquake values, which is expected at a spring sourcing an alluvial aquifer that lacks extensive faulting and connection to a deeper flow circuit.

NER spring, instead, presented lighter isotopic DIC after the earthquake, opposite to the response from the Rieti springs. This could be explained by the position of this spring in the eastern part of the Apennines where there is no deep CO_2 source beneath the aquifer (Figure 1; Chiodini et al., 2004). The shift to lighter values may be caused by ground shaking and increased flow to NER spring inducing more locally derived soil CO_2 to be released into the groundwater.

The stability of $\delta^{34}S_{SO4}$ during and after the seismic sequence suggests that there was no change in source of sulfur to aqueous sulfate (Supporting Information ds01b). The main source of sulfur to the waters, dissolution of Triassic evaporite deposits within the aquifer, has an isotopic signature with $\delta^{34}S_{SO4}$ values ranging from +10 to +20‰ and $\delta^{18}O_{SO4}$ ranging from +5 to +14‰ (Cortecci et al., 2002). Values of $\delta^{18}O_{SO4}$ retained the signature of this source regardless of sulfate concentration, as microbial sulfate reduction has little effect on these waters (Archer et al., 2016; Petitta et al., 2011). The $\delta^{18}O_{SO4}$ of

PES was enriched in samples following the first mainshock (Figure 5b). Most of the oxygen in aqueous sulfate comes from oxygen dissolved from the Triassic evaporites, but up to 25 percent can be from atmospheric oxygen dissolved in groundwater ($\delta^{18}O_{SO4}$ = +23.8‰) (Drever, 2005). There was a significant increase in dissolved oxygen in groundwater of the Gran Sasso aquifer following the 2009 L'Aquila earthquake that has been attributed to a faster flow rate (Galassi et al., 2014). It is possible that the immediate enrichment in PES could be from a faster flow rate and/or new flow paths along earthquake-cleared fractures and dissolving a greater proportion of atmospheric oxygen in groundwater, but this would imply that oxidation of sulfide occurred. This should also have changed $\delta^{34}S_{SO4}$ values, which did not vary, so the observed change in $\delta^{18}O_{SO4}$ of PES remains enigmatic.

5.3. Mechanisms for Transient Increases in Dissolved Ion Concentrations

Various mechanisms have been proposed for transient increases in dissolved ion concentrations after seismic events summarized in Ingebritsen and Manga (2014) and in Table 1. The clearing of fractures and slow-moving water in pore spaces has been invoked in Turkey and Italy after major earthquakes affecting fractured carbonate aquifers (Falcone et al., 2012; Galassi et al., 2014; Pasvanoglu et al., 2004). The movement of deep seated geothermal water and trapped gases has been proposed in Italy (Favara et al., 2001; Italiano et al., 2004: Terakawa et al., 2010, Ciarletti et al., 2016; Barberio et al., 2017) for carbonate affected aquifers, and dilation of stressed aquifers and mixing with other fluids has been proposed in a fractured carbonate aquifer in France (Poitrasson et al., 1999). Changes in water quality of carbonate aquifers caused by strain or rupture of faults has not been documented, but changes in flow have been (Cotecchia et al., 1990).

The stability of the stable isotopes of water and small change in major ions in all springs sampled during the central Italy 2016-17 seismic sequence indicates that mixing with a deep-seated fluid or a fluid with a substantially different composition and origin is not likely. Although the change in $\delta^{13}C_{DIC}$ in two of the Rieti springs indicates the possibility of deep gas contributions, fluid flow of deep seated geothermal fluids to the springs was not observed in the data. The data from the springs sampled indicates that fracture clearing and shaking of fluids from isolated dead-end karstic pore spaces is the likely mechanism for the observed changes (Figure 7). This mechanism was also proposed by Pasvanoglu et al. (2004) after the Mw 7.4 Marmara Earthquake (17 August 1999) in Turkey. They found minor transient changes in flow, turbidity, and major element composition (trace elements were not sampled) in karst marble aquifers used for water supply and suggested that shaking and fracture clearing was the reason for these transient changes. Similarly, Charmoille et al., (2005) also concluded that shaking and fracture/pore space clearing was the cause of water quality changes after the M_L 5.1 earthquake that affected the Fourbanne karst aquifer in eastern France. Although we had no data for turbidity, discussions with the plant operator at Nerea indicated that water became turbid after the 24 August and 26 October 2016 earthquakes (Pierluigi Mariani, pers. comm. 2 November 2016), suggesting a similar clearing of loose material from shaking that occurred after the Marmara Earthquake. More data is needed from carbonate aquifers affected by earthquakes, but these data indicate the importance of local fracture clearing and pore fluid expulsion as the likely mechanism for transient changes in carbonate aquifers after earthquake events. In addition, shaking and fracture clearing may also be understudied and may be important in other rock types affected by earthquakes.

Recently, Barberio et al. (2017) suggested that deep geothermal fluids were the cause of small changes in pH which elevated Cr, As, V and possibly Fe concentrations in springs and a well approximately 70 km south of the central Italy 2016-17 seismic sequence. They suggested that As, V and Cr could be used as precursor indicators of earthquakes because their concentrations rose 4 months prior to the earthquake sequence. They also indicated the increase in these trace element concentrations was caused by a slight lowering of the pH of the solution (by 0.4 pH units), that raised the solubility of these elements. Our data, obtained from springs in a medium radius and in the epicentral area (as in Barberio et al., 2017), indicate that As and V are not good indicators for earthquake activity as they were not detected either before or after the earthquake sequence in any of spring sampled in our study. Cr and Fe did increase after the earthquakes in all the springs measured in our study, but the pre-earthquake data from NER did not show increases before the 24 August 2016 earthquake. In addition, any small changes in pH observed in our study (Supplementary Figure S1) do not correlate with changes in trace element concentrations caused by the earthquakes (Figure 4C).

Although Barbieri et al. (2005) showed that discharge from PES contains approximately 10 percent deep fluid from geothermal sources, our data indicate that indicator geothermal trace elements such as lithium, boron, and arsenic, did not increase during the entire earthquake sequence. If new geothermal water is present, then these geothermal indicator trace elements should also be present and increase (e.g. Bencini et al. 1997), which we do not see in our samples (see supplementary data ds01a). Furthermore, it would take considerable time for geothermal fluids to migrate up through the aquifer. Ages calculated for travel times in these aquifers (see above) are on the time scale of years. If a 4-month precursor window is used, the fluids would have to migrate

from considerable depth (>1 km depth) to the surface in less than 6 months, which doesn't seem plausible. Geothermal water also has a different isotopic composition than atmospherically recharged groundwater. The oxygen isotope composition of geothermal water is more positive relative to hydrogen due to boiling (Truesdell et al. 1977). This would possibly change the isotopic signature after the earthquakes, although this would depend on the volume of geothermal water released.

Taken together, the lack of consistent major element changes and changes in pH, the lack of change in the stable isotopes of water, and the lack of any influx of geothermal indicators (Li, As, V), as well as the rapid transient increase of the trace element concentrations, indicates that at least in the Rieti and Nerea areas, deep-seated geothermal fluids located kilometers below the surface were not responsible for the observed transient changes.

However, the Rieti springs show a component of seismically associated deep-gas release from geothermal or magma sources associated with magma chambers located at depth, as seen in the post-earthquake enrichment of $\delta^{13}C_{DIC.}$

Although our data are not sufficient to provide statistical evidence to confirm or deny the ability of trace elements to be used to predict earthquakes in Italy, the data from the Nerea Spring and bottling plant, suggests that at least in this region, few if any of the chemicals measured were elevated before the earthquake sequence began (Figure 3). In addition, as stated in Ingebritsen and Manga (2014) a wide-range of trace element data and other complementary data would likely be needed to provide useful precursor information because the response to individual earthquakes will depend on many factors that could affect the chemistry of the fluids in an effected aquifer. Unfortunately, much

more work is needed before we can define which are the most useful precursor chemicals in Italy and around the world.

6. Conclusions

Transient changes in the trace element concentrations of springs sampled before and after the central Apennine earthquake sequence from August 2016 to January 2017 show that fractured carbonate aquifers respond more to local shaking that causes fracture and pore fluid clearing than from changes in fluid composition from other sources. This agrees with observations in fractured carbonate aquifers from Turkey and France and may be a predictable mechanism for future seismic response. This study found that both near-field and intermediate-field springs were affected by fault movement and/or ground shaking that induced aquifer pore pressure change, and that these effects were transient in nature during this earthquake sequence. The three large aquifers sourced by these springs are similar in hydrogeologic structure but different in proximity to the ruptured faults. The responses, though notable for both near and intermediate field, were different in duration and onset for each of the three fractured carbonate aquifer springs. These complexities indicate a pore pressure response of aquifers to seismic strain and show the probable role of aquifer hydrogeological structure when considering earthquake effects. The enrichment of $\delta^{13}C_{DIC}$ in PES and SUS following the 2016 main shocks was likely influenced by input of deep-sourced CO_2 gas initiated by movement on faults that serve as conduits, in contrast to the mechanism proposed for other chemical enrichments, where solute-rich groundwater trapped in fractures and closed pore pores with more water-rock interaction time is mixed into fast-flowing groundwater and discharged in a post-seismic pulse.

The lack of change in most of the major ions and in $\delta^{18}O_{H2O}$ and $\delta^{2}H_{H2O}$ after the seismic series indicates that the observed hydrochemical dynamics are the result of within-aquifer changes instead of mixing with another aquifer, geothermal fluids, or aquifer breaching.

These local transient changes, indicate that carbonate aquifers in general respond more to shaking than to input from external fluids. This has important implications for supplying water that may have elevated trace element concentrations to earthquake survivors immediately after earthquakes. In addition, the use of trace element concentrations in aquifers as precursors of imminent earthquakes needs considerably more work to ensure that these predictions are accurate.

Acknowledgements

This work was funded by a RAPID supplement to the National Science Foundation grant GSS-1228126 requested by Paula Noble and Michael Rosen and a University of Insubria grant for the 2016-2017 central Italy seismic sequence requested by Franz Livio. We thank collaborators on related projects who have provided helpful insight; Scott Mensing, Gianluca Piovesan, Fabio Brunamonte, Marco Petitta, David Kreamer. We thank Nerea S.p.A. and Pierluigi Mariani for access to data and samples, and Paolo Bellezza and the "Riserva Naturale dei Laghi Lungo e Ripasottile" for providing access and helping with sampling of the Rieti area springs. In addition, we thank Giorgio Camilloni for providing "emergency" water filters the day after the Amatrice event, Silvia Terrana, Roberto Gambillara, Lorenzo Scibetta, Chiara Frigerio and Franz Livio for help with field work, sampling, and analysis, and to Simon Poulson for isotope analysis and providing helpful guidance to Claire Archer during her PhD studies. Reviews of the manuscript by Alasdair Skelton, Fred Phillips, Michael Manga

and an anonymous reviewer greatly improved the clarity of the manuscript. The US Geological Survey has approved this manuscript for publication. All interpretations reflect the scientific judgment of the authors and do not necessarily reflect the views of their organizations. The use of product names is for identification and does not imply endorsement of the US Government or any of the authors respective organizations. All the data used in this paper are available in the Supplementary Information.

References

Amoruso, A., Crescentini, L., Petitta, M., Rusi, S., & Tallini, M. (2011). Impact of the 6 April 2009 L'Aquila earthquake on groundwater flow in the Gran Sasso carbonate aquifer, Central Italy. *Hydrological Processes, 25* (11), 1754-1764. 10.1002/hyp.7933

Archer, C., Noble, P., Kreamer, D., Piscopo, V., Petitta, M., Rosen, M.R., … & Mensing, S. (2016). Hydrochemical determination of source water contributions to Lake Lungo and Lake Ripasottile (central Italy). *Journal of Limnology*. 10.4081/jlimnol.2016.1576

Banzato, F., Barberio, M. D., Campagnoli, L., Passaretti, S., Pollastrelli, A., Doglioni, C., & Petitta, M. (2017). Groundwater changes in the Nera river valley due to the August-October 2016 seismic sequence in central Italy. (abstract) Flowpath 2017, National Meeting on Hydrogeology, Cagliari, Italy, 14-16 June, 2017, http://convegni.unica.it/flowpath2017/.

Barberio, M. D., Barbieri, M., Billi, A., Doglioni, C., & Petitta, M. (2017). Hydrogeochemical changes before and during the 2016 Amatrice-Norcia seismic sequence (central Italy). *Scientific Reports*, *7*. 10.1038/s41598-017-11990-8

Barbieri, M., Boschetti, T., Petitta, M., Tallini, M. (2005). Stable isotopes (^{2}H, ^{18}O and $^{87}Sr/^{86}Sr$) and hydrochemistry monitoring for groundwater hydrodynamics analysis in a karst aquifer (Gran Sasso, Central Italy). *Applied Geochemistry*, *20* (11) 2063-2081. 10.1016/j.apgeochem.2005.07.008

Barbieri, M., Nigro, A., & Petitta, M. (2017). Groundwater mixing in the discharge area of San Vittorino Plain (Central Italy): geochemical characterization and implication for drinking uses. *Environmental Earth Sciences*, 76(11), 393. 10.1007/s12665-017-6719-1

Bencini, A., Duchi, V., & Martini, M., (1997) Geochemistry of thermal springs of Tuscany (Italy). *Chemical Geology*, 19, 229-252.

Boni, C., Bono, P., & Capelli, G. (1988). Carta Idrogeologica del territorio della Regione Lazio. Scala 1:250.000. Roma, Italy. Special publication Lazio Region.

Cavinato, G. P., & De Celles, P. G. (1999). Extensional basins in the tectonically bimodal central Apennines fold-thrust belt, Italy: response to corner flow above a subducting slab in retrograde motion. *Geology*, *27*(10), 955-958.

Celico, P., De Gennaro, M., Ghiara, M. R., & Stanzione, D. (1981). Variazioni geochimiche nelle acque della valle del Sele dopo l'evento sismico del 23/11/80 in Irpinia. *Rendiconti della Società Geologica Italiana*, 4, 137-139.

Celico, P. (1983). Idrogeologia dei massicci carbonatici, delle piane quaternarie e delle aree vulcaniche dell'Italia centro-meridionale (Marche e Lazio meridionale, Abruzzo, Molise e Campania). *Quaderni CASMEZ*, 4/2, Roma.

Cello, G., Mazzoli, S., Tondi, E., & Turco, E. (1997). Active tectonics in the central Apennines and possible implications for seismic hazard analysis in peninsular Italy. *Tectonophysics*, *272*(1), 43-68. 10.1016/S0040-1951(96)00275-2

Centamore, E., Fumanti, F., & Nisio, S. (2002). The central-northern Apennines geological evolution from Triassic to Neogene time. Bollettino della Società Geologica Italiana, Vol. Spec., 1, 181-197.

Charmoille, A., Fabbri, O., Mudry, J., Guglielmi, Y., Bertrand C. (2005) Post-seismic permeability change in a shallow fractured aquifer following a ML 5.1 earthquake (Fourbanne karst aquifer, Jura outermost thrust unit, eastern France). *Geophysical Research Letters*, 32: L18406. 10.1029/2005GL023859.

Checcucci, R., Mastrorillo, L., & Valigi, D. (2017). Acque sotterranee e terremoti: alcune considerazioni sugli effetti della sismicità sulla disponibilità della risorsa idrica in Valnerina. *Acque Sotterranee-Italian Journal of Groundwater*, 6(1). 10.7343/as-2017-259

Chiaraluce, L., Di Stefano, R., Tinti, E., Scognamiglio, L., Michele, M., Casarotti, E., ... & Lombardi, A. (2017). The 2016 central Italy seismic sequence: A first look at the mainshocks, aftershocks, and source models. *Seismological Research Letters*, *88*(3), 757-771. 10.1785/0220160221

Chiodini, G., Frondini, F., Cardellini, C., Parello, F., & Peruzzi, L. (2000). Rate of diffuse carbon dioxide Earth degassing estimated from carbon balance of regional aquifers: the case of central Apennine, Italy. *Journal of Geophysical Research: Solid Earth*, *105*(B4), 8423-8434. 10.1029/1999JB900355

Chiodini, G., Cardellini, C., Amato, A., Boschi, E., Caliro, S., Frondini, F., & Ventura, G. (2004). Carbon dioxide Earth degassing and seismogenesis in central and southern Italy. *Geophysical Research Letters*, *31*(7).10.1029/2004GL019480

Civico R., Pucci, S., Villani, F., Pizzimenti, L., De Martini, P.M., Nappi, R., & the Open EMERGEO Working Group (2017). Surface ruptures following the 30 October 2016 Mw 6.5 Norcia earthquake, central Italy. *Journal of Maps*, in press, DOI: 10.1080/17445647.2018.1441756.

Ciarletti, M., Plastino, W., Peresan, A., Nisi, S., Copia, L., Panza, G. F., & Povinec, P. P. (2016). Uranium Groundwater Monitoring and Seismic Analysis: A Case Study of the Gran Sasso Hydrogeological Basin, Italy. *Pure and Applied Geophysics*, *173*(4), 1079–1095. 10.1007/s00024-015-1152-4

Civita, M. V., & Fiorucci, A. (2010). The recharge-discharge process of the Peschiera spring system (central Italy). *Aqua Mundi*, *1*, 161-178.

Claesson, L., Skelton, A., Graham, C., Dietl, C., Mörth, M., Torssander, P., & Kockum, I. (2004). Hydrogeochemical changes before and after a major earthquake. *Geology*, *32*(8), 641-644. 10.1130/G20542.1

Cortecci, G., Dinelli, E., Bencini, A., Adorni-Braccesi, A., & La Ruffa, G. (2002). Natural and anthropogenic SO_4 sources in the Arno river catchment, northern Tuscany, Italy: a chemical and isotopic reconnaissance. *Applied Geochemistry*, *17*(2), 79-92. 10.1016/S0883-2927(01)00100-7

Costantini, E. A., Fantappié, M., & L'Abate, G. (2013). Climate and pedoclimate of Italy. In *The Soils of Italy* (pp. 19-37). Springer Netherlands. 10.1007/978-94-007-5642-7_2

Cotecchia, V., Salvemini, A., & Ventrella, N. A. (1990). Interpretazione degli abbassamenti territoriali indotti dal terremoto del 23 Novembre 1980 e correlazioni con i danni osservati su talune strutture ingegneristiche dell'area epicentrale irpina. *Rivista Italiana Di Geotecnica*, *24*(4), 145-158.

Drever, J. I. (Ed.). (2005). *Surface and Ground Water, Weathering, and Soils: Treatise on Geochemistry* (Vol. 5). Elsevier.

Falcone, R. A., Carucci, V., Falgiani, A., Manetta, M., Parisse, B., Petitta, M., ... & Tallini, M. (2012). Changes on groundwater flow and hydrochemistry of the Gran Sasso carbonate aquifer after 2009 L'Aquila earthquake. *Italian Journal of Geosciences*, *131*(3), 459-474. 10.3301/IJG.2011.34

Favara, R., Italiano, F., & Martinelli, G. (2001). Earthquake-induced chemical changes in the thermal waters of the Umbria region during the 1997–1998 seismic swarm. *Terra Nova*, *13*(3), 227–233. 10.1046/j.1365-3121.2001.00347.x

Fusari, A., Carroll, M. R., Ferraro, S., Giovannetti, R., Giudetti, G., Invernizzi, C., ... & Pennisi, M. (2017). Circulation path of thermal waters within the Laga foredeep basin inferred from chemical and isotopic ($\delta^{18}O$, δD, ^{3}H, $^{87}Sr/^{86}Sr$) data. *Applied Geochemistry*, *78*, 23-34. 10.1016/j.apgeochem.2016.11.021

Galassi, D. M., Lombardo, P., Fiasca, B., Di Cioccio, A., Di Lorenzo, T., Petitta, M., & Di Carlo, P. (2014). Earthquakes trigger the loss of groundwater biodiversity. *Scientific reports*, *4*, 6273. 10.1038/srep06273

Giustini, F., Brilli, M., & Patera, A. (2016). Mapping oxygen stable isotopes of precipitation in Italy. *Journal of Hydrology: Regional Studies*, *8*, 162-181. 10.1016/j.ejrh.2016.04.001

Guerrieri L., V. Comerci, L. Ferreli, R. Pompili, L. Serva, F. Brunamonte, Michetti A.M., 2006, Geological evolution of the intermountain Rieti basin (Central Appennines), In: G. Pasquarè, C. Venturini and G. Groppelli (Eds.), "Mapping Geology in Italy", 123-130 (2004), APAT – Servizio Geologico d'Italia, Printed by SELCA, Firenze.

Hartmann, J., & Levy, J. K. (2006). The influence of seismotectonics on precursory changes in groundwater composition for the 1995 Kobe earthquake, Japan. *Hydrogeology Journal*, *14*(7), 1307-1318. 10.1007/s10040-006-0030-7

Ingebritsen, S. E., & Manga, M. (2014). Earthquakes: hydrogeochemical precursors. *Nature Geoscience*, *7*(10), 697. 10.1038/ngeo2261

INGV Istituto Nazionale di Geofisica e Vulcanologia, earthquake database: http://cnt.rm.ingv.it/en/ (accessed August 2017)

Italiano, F., Martinelli, G., & Rizzo, A. (2004). Geochemical evidence of seismogenic-induced anomalies in the dissolved gases of thermal waters: A case study of Umbria (Central Apennines, Italy) both during and after the 1997–1998 seismic swarm. *Geochemistry, Geophysics, Geosystems*, *5*(11), Q11001. 10.1029/2004GC000720

La Vigna, F., Carucci, V., Mariani, I., Minelli, L., Pascale, F., Mattei, M., ... & Tallini, M. (2012). Intermediate-field hydrogeological response induced by L'Aquila earthquake: the Acque Albule hydrothermal system (Central Italy). *Italian Journal of Geosciences*, *131*(3), 475-485. 10.3301/IJG.2012.05

Longinelli, A., & Selmo, E. (2003). Isotopic composition of precipitation in Italy: a first overall map. *Journal of Hydrology*, *270*(1), 75-88. 10.1016/S0022-1694(02)00281-0

Malakootian, M., & Nouri, J. (2010). Chemical Variations of Ground Water Affected by the Earthquake in Bam region. *International Journal of Environmental Research*, *4*(3), 443-454.

Manga, M., & Wang, C. Y. (2015). 4.12. Earthquake hydrology. *Treatise on Geophysics, second edition. Elsevier, Oxford*, 305-328.

Martarelli, L., Petitta, M., Scalise, A., & Silvi, A. (2008). Cartografia idrogeologica sperimentale della Piana Reatina (Lazio). *Memorie Descrittive della Carta Geologica d'Italia*, *81*, 137-156.

Mastrorillo, L., & Petitta, M. (2014). Hydrogeological conceptual model of the upper Chienti River Basin aquifers (Umbria-Marche Apennines). *Italian Journal of Geosciences*, *133*(3), 396-408. 10.3301/IJG.2014.12

Morettini, E., Santantonio, M., Bartolini, A., Cecca, F., Baumgartner, P. O., & Hunziker, J. C. (2002). Carbon isotope stratigraphy and carbonate production during the Early–Middle Jurassic: examples from the Umbria–Marche–Sabina Apennines (central Italy). *Palaeogeography, Palaeoclimatology, Palaeoecology*, *184*(3), 251-273. 10.1016/S0031-0182(02)00258-4

Morgantini, N., Frondini, F., & Cardellini, C. (2009). Natural trace elements baselines and dissolved loads in groundwater from carbonate aquifers of central Italy. *Physics and Chemistry of the Earth, Parts A/B/C*, *34*(8), 520-529. 10.1016/j.pce.2008.05.004

Nanni, T., & Rusi, S. (2003). Idrogeologia del massiccio carbonatico della montagna della Majella (Appennino centrale). *Bollettino della Società Geologica Italiana*, *122*(2), 173-202.

Pasvanoglu, S., Canik, B., & Rosen, M. R. (2004). Hydrogeology and Possible Effects of the Mw 7.4 Marmara Earthquake (17 August 1999) on the Spring Waters in the Orhangazi-Bursa Area, Hirkey. *Geological Society of India*, *63*(3), 313-322.

Petitta, M., Primavera, P., Tuccimei, P., & Aravena, R. (2011). Interaction between deep and shallow groundwater systems in areas affected by Quaternary tectonics (Central Italy): a geochemical and isotope approach. *Environmental Earth Sciences*, *63*(1), 11-30. 10.1007/s12665-010-0663-7

Petitta, M., Mastrorillo, L., Preziosi, E., Banzato, F., Barberio, M.D., ... & Doglioni, C. (2018) Water-table and discharge changes associated with the 2016–2017 seismic sequence in central Italy: hydrogeological data and a conceptual model for fractured carbonate aquifers. *Hydrogeology Journal* https://doi.org/10.1007/s10040-017-1717-7

Pieri, M. (1966). Tentativo di ricostruzione paleogeografico-strutturale dell'Italia centro-meridionale. *Geologica Romana 5*(4), 407-424.

Pizzi, A., Di Domenica, A., Gallovič, F., Luzi, L., & Puglia, R. (2017). Fault segmentation as constraint to the occurrence of the main shocks of the 2016 Central Italy seismic sequence. *Tectonics*, 36, 2370–2387. https://doi.org/10.1002/2017TC004652

Poitrasson, F., Dundas, S. H., Toutain, J.-P., Munoz, M., & Rigo, A. (1999). Earthquake-related elemental and isotopic lead anomaly in a springwater. *Earth and Planetary Science Letters*, *169*(3), 269–276. 10.1016/S0012-821X(99)00085-0

Quattrocchi, F. (1999). In search of evidence of deep fluid discharges and pore pressure evolution in the crust to explain the seismicity style of the Umbria-Marche 1997-1998 seismic sequence (Central Italy). *Annals of Geophysics*, *42*(4), 609-636

Raco, B., Dotsika, E., Feroni, A. C., Battaglini, R., & Poutoukis, D. (2013). Stable isotope composition of Italian bottled waters. *Journal of Geochemical Exploration*, *124*, 203-211. 10.1016/j.gexplo.2012.10.003

Reddy, D. V., Nagabhushanam, P., & Sukhija, B. S. (2011). Earthquake (M 5.1) induced hydrogeochemical and δ18O changes: validation of aquifer breaching—mixing model in Koyna, India. *Geophysical Journal International*, *184*(1), 359-370. 10.1111/j.1365-246X.2010.04838.x

Roberts, G. P., & Michetti, A. M. (2004). Spatial and temporal variations in growth rates along active normal fault systems: an example from The Lazio–Abruzzo Apennines, central Italy. *Journal of Structural Geology*, *26*(2), 339-376. 10.1016/S0191-8141(03)00103-2

Skelton, A., Claesson, L., Chakrapani, G., Mahanta, C., Routh, J., Mörth, M. & Khanna, P. (2008). Coupling Between Seismic Activity and Hydrogeochemistry at the Shillong Plateau, Northeastern India. *Pure Applied Geophysics*, *165* (1), 45–61. 10.1007/s00024-007-0288-2

Skelton, A., Andrén, M., Kristmannsdóttir, H., Stockmann, G., Mörth, C. M., Sveinbjörnsdóttir, Á., ... & Siegmund, H. (2014). Changes in groundwater chemistry before two consecutive earthquakes in Iceland. *Nature Geoscience*, *7*(10), 752-756. 10.1038/ngeo2250

Spadoni, M., Brilli, M., Giustini, F., & Petitta, M. (2010). Using GIS for modelling the impact of current climate trend on the recharge area of the S. Susanna spring (central Apennines, Italy). *Hydrological Processes*, *24*(1), 50-64. 10.1002/hyp.7452

Tarragoni, C. (2006). Determinazione della "quota isotopica" del bacino di alimentazione delle principali sorgenti dell'alta Valnerina. *Geologica Romana, 39*, 55-62.

Terakawa, T., Zoporowski, A., Galvan, B., & Miller, S. A. (2010). High-pressure fluid at hypocentral depths in the L'Aquila region inferred from earthquake focal mechanisms. *Geology*, *38*(11), 995-998. 10.1130/G31457.1

Ufficio Idrografico e Mareografico, Regione Lazio (2017). Pluviometric data retrieved from: http://www.idrografico.roma.it/annali/ (accessed June 6 2017)

Truesdell, A.H., Nathenson, M., & Rye, R.O. (1977). The Effects of Subsurface Boiling and Dilution on the Isotopic Compositions of Yellowstone Thermal Waters. *Journal of Geophysical Research, 82*(26), 3694-3704.

Valigi, D., Cambi, C., Mastrorillo, L., Barchi, M. R., Cardellini, C., Checcucci, R., ... & Vispi, I. (2017). Discharge variations of springs induced by strong earthquakes: the case of the mw 6.5 Norcia event (Italy, October 30 th 2016). (abstract) "Flowpath 2017" National Meeting on Hydrogeology, Cagliari, Italy, 14-16 June, 2017, http://convegni.unica.it/flowpath2017/.

Vittori E., Deiana, G., Esposito, E., Ferreli, L., Marchegiani, L., Mastrolorenzo, G., … & Tondi, E., 2000, Ground effects and surface faulting in the September-October 1997 Umbria-Marche (Central Italy) seismic sequence. *Journal of Geodynamics*, 29, 535-564. doi.org/10.1016/S0264-3707(99)00056-3

Vittori, E., Di Manna, P., Blumetti, A. M., Comerci, V., Guerrieri, L., Esposito, E., ... & Berlusconi, A. (2011). Surface faulting of the 6 April 2009 Mw 6.3 L'Aquila earthquake in central Italy. *Bulletin of the Seismological Society of America*, *101*(4), 1507-1530. 10.1785/0120100140

Woith, H., Wang, R., Maiwald, U., Pekdeger, A., & Zschau, J. (2013). On the origin of geochemical anomalies in groundwaters induced by the Adana 1998 earthquake. *Chemical Geology*, *339*, 177-186. 10.1016/j.chemgeo.2012.10.012

A1. Appendix: Detailed Methods

A1.1. Field Sampling Operations

The physio-chemical parameters of pH, temperature and electrical conductivity (EC) were evaluated on site using specific field probes: a HANNA Instruments (USA) HI 9025 pH-meter equipped with sensors for pH and temperature and a HANNA Instruments HI 9033 conductivity probe for electrical conductivity. Hardness and alkalinity were directly evaluated on site using MERCK (Germany) titration kits. All field sampling and analysis procedures were made wearing nitrile gloves to avoid contamination during sampling.

All LPDE bottles used were pre-washed using NALGENE L900 (USA) soap. Sample bottles were rinsed three times with the water to be collected before being filled. Samples for laboratory analysis were filtered on site with a 0.45 micrometer sterile Millex-GS millipore MCE membrane and transferred to LPDE bottles that had been additionally pre-washed with 2% HNO_3; 1x for cation analyses, and 2x for isotope and trace element analyses.

A1.2. Ionic Chromatography

Major anions and cations were analyzed using a Metrohm (Swiss Confederation) EcoIC instrument with different settings for cations and anions analyses. Samples for anions were analyzed using a Metrosep A Supp 5-250 column and a solution of 3.2 mM

Na_2CO_3 and 1 mM $NaHCO_3$ as eluent, following EPA method 300.0 (Pfaff, 1993). Samples for cations were analyzed using a Metrosep C4-150 column and 5 mM H_3PO_4 as eluent. Cations samples, moreover, were acidified with 100 ml of 1M HNO_3 to reach a pH value of ca. 2 (Jackson, 2000). The limit of detection (LOD) of the technique was calculated as 0.05 ppm. Ionic balances were calculated to assess data reliability following the equation (1):

$$(\sum cations-\sum anions)/(\sum cations+\sum anions) \quad (1)$$

Where cations and anions concentrations are expressed as milliequivalent per liter (Chapra, 2008). Ionic balances were less than ±10% for almost all the samples, except for 3 samples analyzed in Archer et al. (2016), and in 60% of the samples ionic balances were below ± 5%. (Supporting Information ds01a).

A1.3. Inductively Coupled Plasma Mass Spectrometry (ICP-MS)

Samples for trace element analysis were acidified with 2% ultrapure HNO_3, previously obtained by sub-boiling distillation of 65% acid using Milestone (USA) duoPUR. The samples were then analyzed using a Thermo scientific (USA) Icap Q instrument. To certify the quality of analysis and observe possible instrumental bias, an internal standard with 10 ppb of indium (In) was spiked in all the samples. The recovery of In spikes were all within 10% of the value of the spiked added. Elements chosen for the analysis were Li, B, Al, Cr, Mn, Co, Cu, Ni, Fe, Pb, U, Rb, and Sr. Errors estimated by replicate analysis were lower than ± 0.01 ppb for Cr, Mn, Pb, U, Rb and Sr. Error for Li, Al, and Fe was ± 0.2 ppb, for Ni was ±0.03 ppb, and for Cu was ± 0.5 ppb. Other

elements (Se, As, Cd, V) were analyzed to see possible release after the earthquake, but the concentrations detected were equal to or lower than our LOD values (table A1) and showed no discernable change: for this reason, these elements are not reported. Li and B were analyzed in most samples, and also did not show significant changes. Boron analyses were conducted using a platinum injector and a plastic nebulizer to avoid contamination from borosilicate glass. Samples were stored in plastic bottles. A sample of the acid used to preserve samples in the laboratory was also analyzed. Although the acid blanks do contain low concentrations of the trace elements analyzed, they are below the concentrations of the lowest environmental samples. Concentrations presented in this paper have not been corrected to exclude this low-level contamination (Supporting Information ds01a). The pre-earthquake ICP-MS analyses for PES, SUS and VIC were performed using archived waters collected during the previous study of Archer et al. (2016). These waters were sampled using the same procedure and were preserved with nitric acid. All ionic chromatography and ICP-MS analyses were performed at the Università degli Studi Dell'Insubria Dipartimento di Scienza e Alta Tecnologia, Como, Italy.

	µg/L
Li	**0.08300**
B	**0.02568**
Al	0.05350
V	0.00070
Cr	0.00310
Mn	0.00216
Fe	0.01888
Co	0.00024
Ni	0.00475
Cu	0.00105
As	0.00181
Se	0.00199
Rb	0.00151

Sr	0.00115
Cd	0.00042
Pb	0.00021
U	0.00002

Table A1: Limit Of detection of ICP-MS instrument for the analyzed metals.

A1.4. Isotope Analysis

Waters were prepared for isotopic analysis by precipitation of dissolved sulfate as $BaSO_4$ following the method of Carmody et al. (1998). $BaSO_4$ precipitates were analyzed for $\delta^{34}S_{SO4}$ using V_2O_5 as a combustion aid, and followed the methods of Giesemann et al. (1994). $BaSO_4$ precipitates were analyzed for $\delta^{18}O_{SO4}$ following the method of Kornexl et al. (1999). The analytical error (1-sigma), estimated by replicate analysis, was ±0.2‰ and ±0.4 ‰ for $\delta^{34}S_{SO4}$ and $\delta^{18}O_{SO4}$, respectively. Water samples were prepared for isotopic analysis of dissolved inorganic carbon by precipitation as $SrCO_3$ after the method of Usdowski et al. (1979), and then analyzed using the method of Harris et al. (1997), with analytical error within ±0.2‰. Waters were analyzed for $\delta^{18}O_{H2O}$ using the CO_2 - H_2O equilibration method of Epstein and Mayeda (1953), and for $\delta^{2}H_{H2O}$ using the method of Morrison et al. (2001). The analytical error of these measurements was ±0.1‰ and ±1.0 ‰ for $\delta^{18}O_{H2O}$ and $\delta^{2}H_{H2O}$, respectively. All stable isotope analyses were carried out at the University of Nevada, Reno Stable Isotope lab. All values are reported using delta notation (δ‰), and the standards used were V-SMOW for oxygen and hydrogen, V-PDB for carbon and V-CDT for sulfur. Between 5 and 10% of all analyses were run as replicates to determine reproducibility of the results. All replicates were within 10% of the original value.

A1.5. Meteorological and Seismological Data Compilation

Daily precipitation and temperature measured at Peschiera spring, Mt. Terminillo (for SUS, VIC and PES) and Leonessa (for NER) was retrieved from http://www.idrografico.roma.it/annali/ (2017). The monthly total precipitation amounts were calculated for the sampled months (Supporting Information ds01d). Dates, location, and magnitudes of earthquakes in the seismic sequence were mapped from the INGV (Istituto Nazionale di Geofisica e Vulcanologia) Centro Nazionale Terremoti database, http://cnt.rm.ingv.it/en/.

A1.6. Quantitative Analyses

The means and standard deviation of the pre-earthquake data were calculated to demonstrate a range of natural variability. The potential correlations among trace element concentrations were analyzed using the Pearson correlation coefficient and r^2 values. Compiled monthly precipitation data was also included in these tests to determine if meteorological parameters had any control on concentrations of dissolved constituents. The correlation matrices were generated using the total monthly precipitation of the month prior to the samplings date. All sampling dates were then tested for correlation with all trace elements and the prior months' precipitation.

As an initial data analysis step, all hydrochemical data were plotted in time series by spring to check for variations outside the mean pre-earthquake values. A Principal Component Analysis (PCA) of elemental data was then performed to better evaluate covariance of elements and to establish the temporal response by plotting eigenvalues in time series. This data reduction technique applies a linear combination of the analyzed variables to obtain new uncorrelated variables representing the maximum variance of the

dataset, defined as principal components (Kramer, 1998). Data used in the PCA were first scaled and centered by the mean, using the following equation (2):

$x_i' = \frac{x_i - \mu}{s}$ (2)

Where μ is the mean, s is the standard deviation, x_i is the original value and x_i' is the standardize value (Kramer, 1998). PCA was performed using the STATISTICA 7 software, using a correlation matrix (Statsoft, inc., 2007). PCA was applied to samples before and after the earthquake, in all the sampled springs, only for samples were major ions and trace elements were analyzed.

Methods References

Archer, C., Noble, P., Kreamer, D., Piscopo, V., Petitta, M., Rosen, M.R., Poulson, S.R., Piovesan, G., & Mensing, S. (2016). Hydrochemical determination of source water contributions to Lake Lungo and Lake Ripasottile (central Italy). *Journal of Limnology*. 10.4081/jlimnol.2016.1576

Carmody, R.W., Plummer, L.N., Busenberg, E., & Coplen, T.B. (1998). Methods for collection of dissolved sulfate and sulfide and analysis of their sulfur isotopic composition. U.S. Geological Survey, Open-File Report 97-234: 91 p.

Chapra, S. C. (2008). *Surface water-quality modeling*. Waveland press. 784 p.

Epstein, S., & Mayeda, T. (1953). Variation of O18 content of waters from natural sources. *Geochimica et cosmochimica acta*, *4*(5), 213-224. 10.1016/0016-7037(53)90051-9

Giesemann, A., Jäger, H. J., Norman, A. L., Krouse, H. R., & Brand, W. A. (1994). Online sulfur-isotope determination using an elemental analyzer coupled to a mass spectrometer. *Analytical Chemistry*, *66*(18), 2816-2819. 10.1021/ac00090a005

Harris, D., Porter, L. K., & Paul, E. A. (1997). Continuous flow isotope ratio mass spectrometry of carbon dioxide trapped as strontium carbonate. *Communications in Soil Science & Plant Analysis*, *28*(9-10), 747-757. 10.1080/00103629709369827

Jackson, P. E. (2000). Ion Chromatography in Environmental Analysis In Jackson, P. E., *Encyclopedia of Analytical Chemistry*. *New Jersey*, John Wiley & Sons, (pp. 1-20). 10.1002/9780470027318.a0835

Kornexl, B. E., Gehre, M., Höfling, R., & Werner, R. A. (1999). On-line d18O measurement of organic and inorganic substances. *Rapid Communications in Mass Spectrometry*, *13*(16), 1685-1693.

Kramer, R. (1998). *Chemometric techniques for quantitative analysis*. Boca Raton, FL: CRC Press.

Morrison, J., Brockwell, T., Merren, T., Fourel, F., & Phillips, A. M. (2001). On-line high-precision stable hydrogen isotopic analyses on nanoliter water samples. Analytical Chemistry, v. 73, (15), 3570-3575. 10.1021/ac001447t

Pfaff, J. D. (1993). Determination of inorganic anions by ion chromatography. (EPA method 300.0) Washington, DC: United States Environmental Protection Agency https://www.epa.gov/sites/production/files/2015-08/documents/method_300-0_rev_2-1_1993.pdf

StatSoft, Inc. (2007). STATISTICA (data analysis software system), version 8.0. www.statsoft.com.

Usdowski, E., Hoefs, J., & Menschel, G. (1979). Relationship between13C and18O fractionation and changes in major element composition in a recent calcite-depositing spring—A model of chemical variations with inorganic CaCO3 precipitation. *Earth and Planetary Science Letters*, *42*(2), 267-276. 10.1016/0012-821X(79)90034-7

Table

Table 1. Major changes documented from different mechanisms of movement after earthquakes in fractured carbonate aquifers. An "L" or "T" marked in the column indicates statistically significant changes in the constituent from pre-earthquake conditions. L = lasting changes, T = temporary changes, ND = not documented in literature; either as no change, or not measured.

Mechanism of water quality changes after earthquake	***Flow***	***Major ions***	***Trace elements***	***^{2}H and ^{18}O of water***	***^{34}S and ^{18}O of dissolved sulfate***	***^{13}C of DIC***	***References***
Strain/rupture of faults	L or T	ND	ND	ND	ND	ND	(Cotecchia et al., 1990; Petitta et al., 2018)
Near surface dilation and shaking	T	T	T	ND	ND	ND	(Charmoille et al., 2005; Pasvanoglu et al., 2004)
dilation and mixing of different aquifers	T	T	T	ND	ND	ND	(Poitrasson et al., 1999)
Release of deep-seated geothermal fluids	L or T	L or T	L or T (inclusion of geothermal trace elements such as Li, B, and As should also occur, but not reported)	ND	ND	ND	(Barberio et al., 2017)
Release of deep-seated trapped gases	--	T	T (data available only for U)	ND	ND	L or T	(Ciarletti et al., 2016; Favara et al., 2001; Italiano et al.,

						2004)

Figures

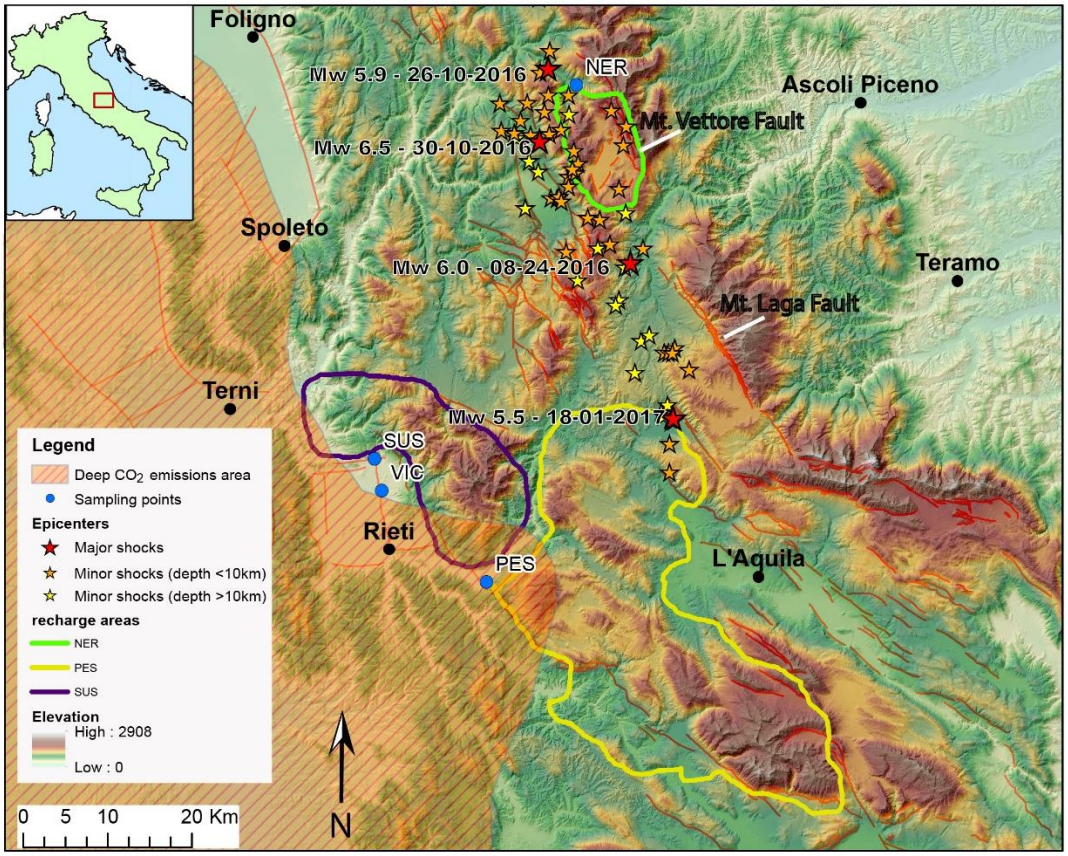

Figure 1. Locality map. Red lines indicate active faults (from ITHACA database, http://sgi.isprambiente.it/geoportal/catalog/content/project/ithaca.page). Red stars indicate earthquake mainshocks, from north to south: 26 October 2016 (42.9087, 13.1288), 30 October 2016 (42.8322, 13.1107), 24 August 2016 (42.6983, 13.2335), January 18th, 2017. Orange and yellow stars indicate aftershocks with magnitude greater than 4.0. Orange denotes depths <10 km, Yellow denotes depths >10 km. The blue circles indicate locations of springs sampled, from north to south: Nerea Spring (NER), St. Susanna Spring (SUS), Vicenna Riara Spring (VIC), and Peschiera Spring (PES). The purple outline indicates the SUS recharge area (Spadoni et al. 2010), the yellow outline indicates PES (Civita & Fiorucci 2010), and the green outline denotes NER recharge area

(Tarragoni 2006). The outline of the deep CO_2 emissions area (hashed orange area) is adopted from (Chiodini et al., 2004). Earthquake Data from: INGV, ISIDe working group (2016) version 1.0, DOI: 10.13127/ISIDe.

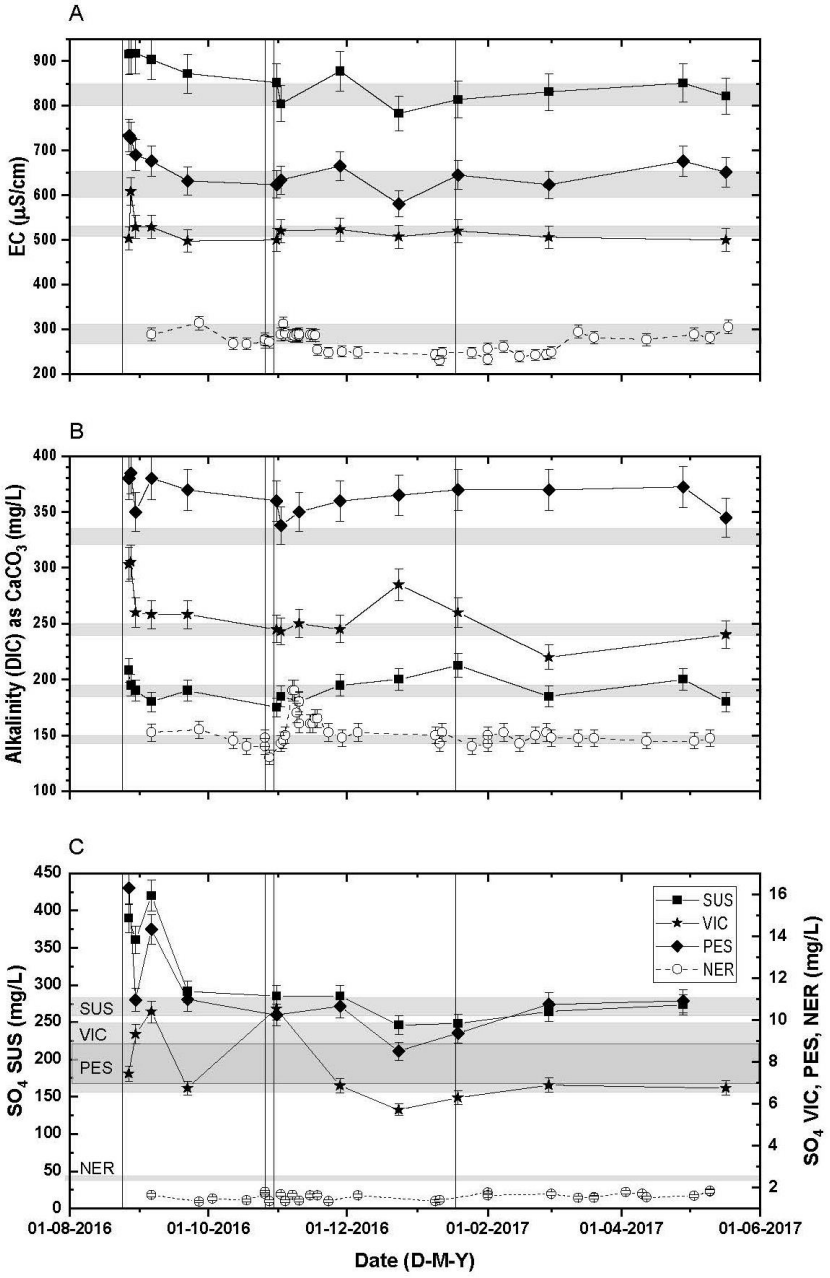

Figure 2. Time series plots of A) Electrical conductivity (EC), from SUS, VIC, PES, and NER. B) alkalinity (mg/L as $CaCO_3$), and C) sulfate concentrations. The vertical black lines indicate earthquake mainshocks (24 August, 2016; 26 October 2016; 30 October

2016; 18 January 2017), horizontal shaded fields indicate the pre-earthquake ranges for each spring.

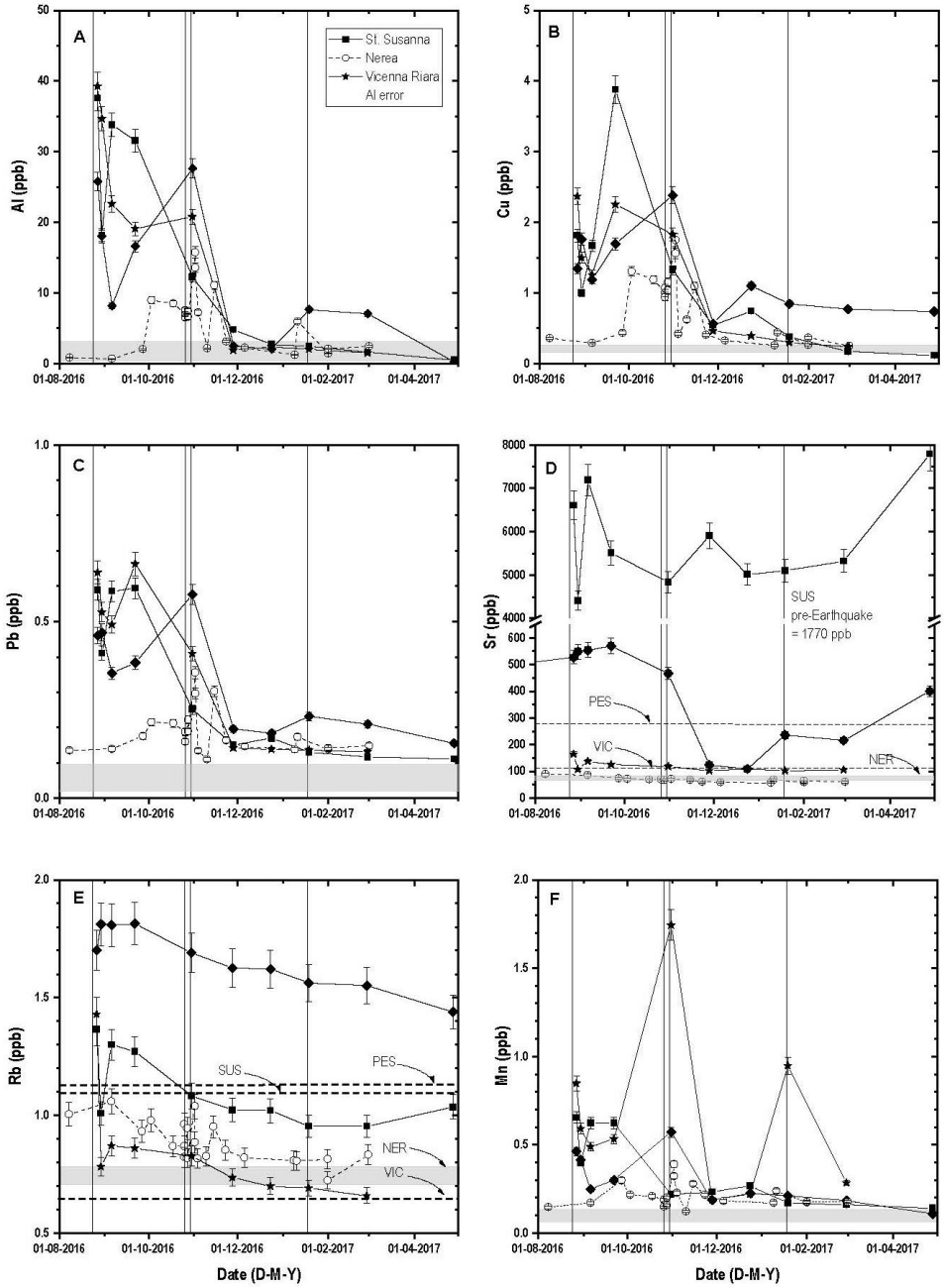

Figure 3. Time series plots of trace metals: A) Aluminum (Al) B), Copper (Cu) C), Lead (Pb) D), Strontium (Sr) E), Rubidium (Rb) and F) Manganese (Mn) at SUS, VIC, PES, and NER. Vertical black lines indicate earthquake mainshocks (24 August, 2016; 26 October 2016; 30 October 2016; 18 January 2017), horizontal gray fields indicate the pre-

earthquake range of values for Al, Cu, Pb, and Mn, where all springs had the same range. The plots of Sr and Rb have dashed horizontal lines to indicate the pre-earthquake values at each individual spring. The pre-earthquake concentration of Sr at SUS (1770 ppb) is not visible on the graph due to the Y-axis break.

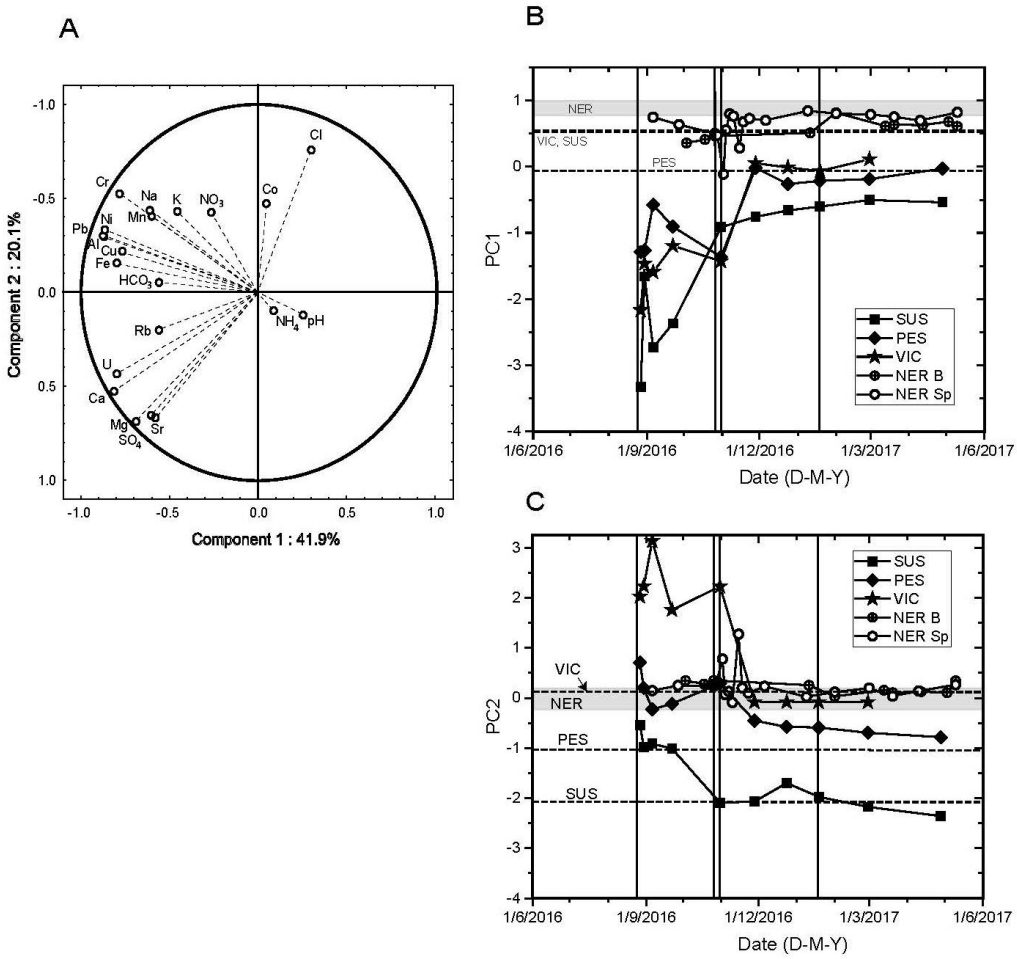

Figure 4: A) Loading plot of PCA components 1 and 2 (explaining 62% of the total variance). Metals as Pb, Al, Ni, Cu, Cr, Mn, Fe are highly correlated in all the sampled springs. B) Time series of PC1 showing variance over time in relation to the major earthquakes (black vertical lines; (24 August, 2016; 26 October 2016; 30 October 2016; 18 January 2017)) Higher numbers show more variance. C) Time series of PC2 variance in relation to the major earthquakes (black vertical lines). The spring and bottling plant

samples are separated here into NER B for bottling plant, and NER Sp for samples from the spring.

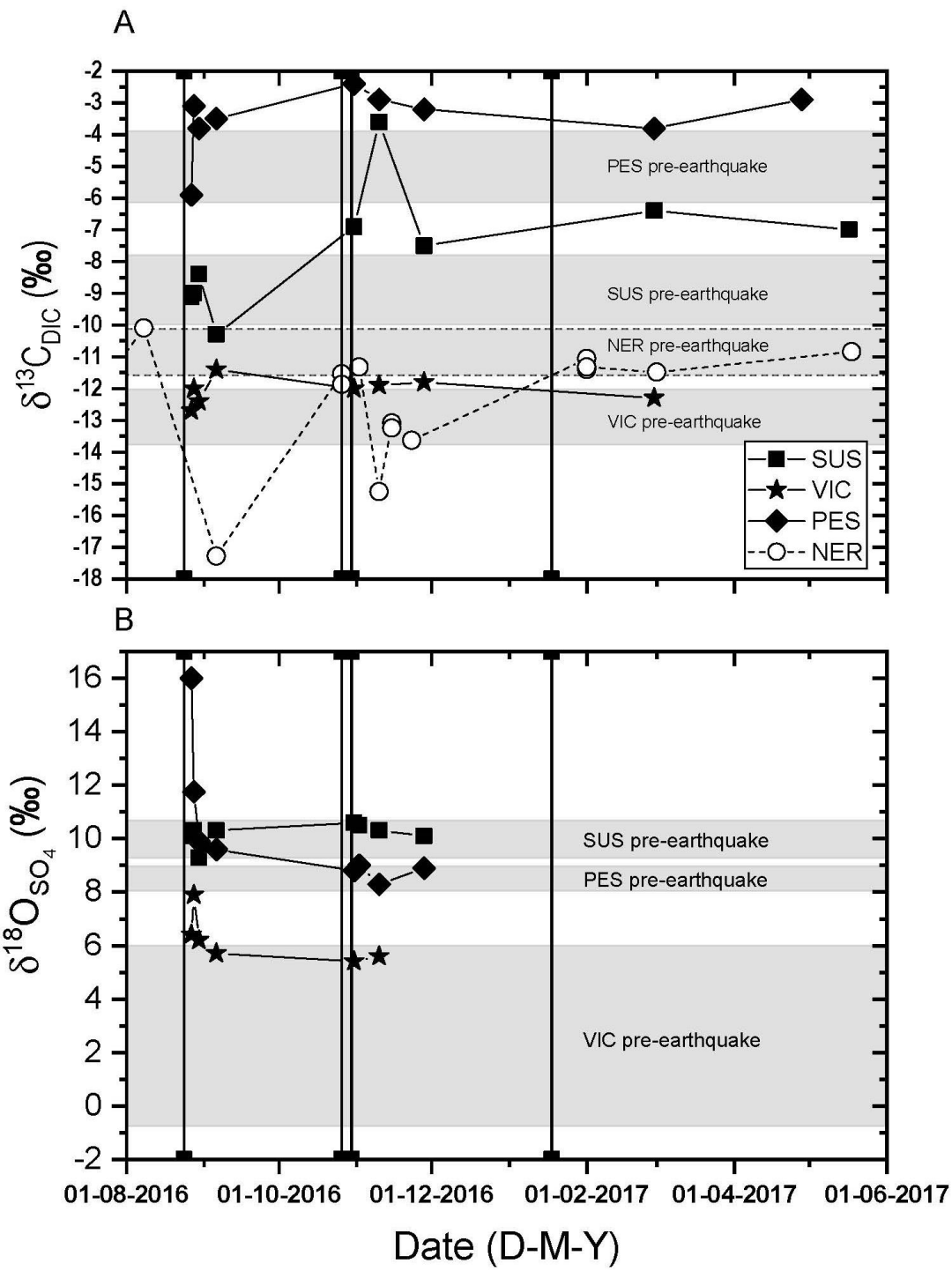

Figure 5: Time series plots of a) $\delta^{13}C_{DIC}$ and b) $\delta^{18}O_{SO4}$ during the earthquake sequence. Shaded bars pre-earthquake values each spring. No $\delta^{18}O_{SO4}$ values are available for NER because sulfate concentrations were too low to get a usable amount of sulfate from archived water samples. Vertical black lines indicate earthquake mainshocks (24 August, 2016; 26 October 2016; 30 October 2016; 18 January 2017).

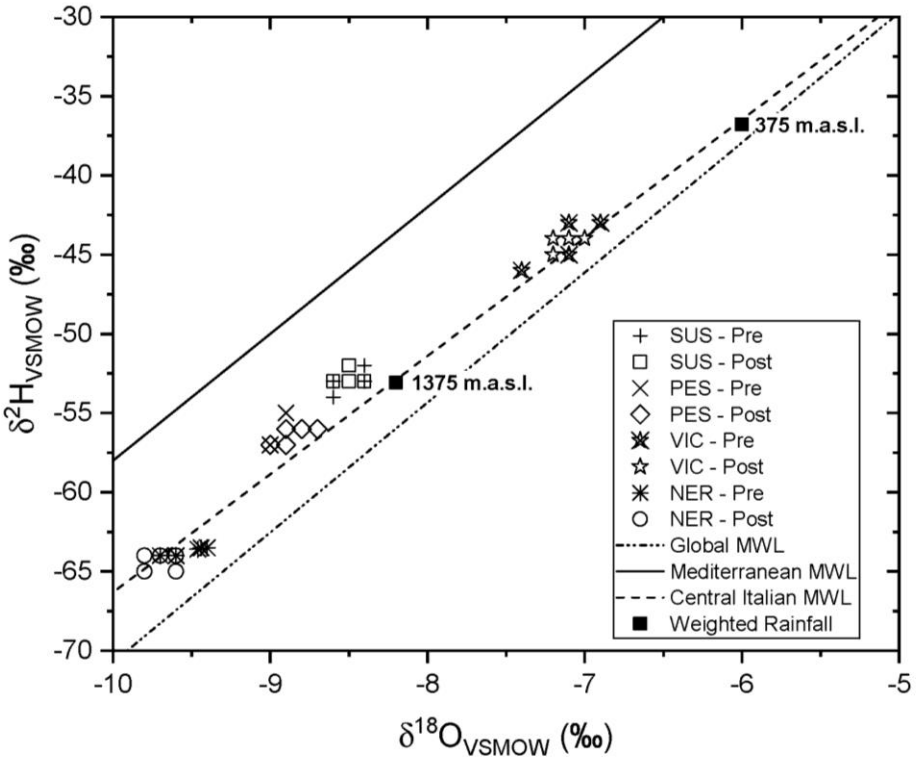

Figures 6, Stable isotopes of water from springs pre- and post- earthquake compared to global, central Italian, and Mediterranean meteoric water lines; GMWL, cIMWL, and MMWL, respectively. Equations for cIMWL is from Longinelli and Selmo (2003) and rain-gauge measurements at 2 elevations in the central Apennines (375, 1375 m a.s.l) is from Spadoni et al. (2010).

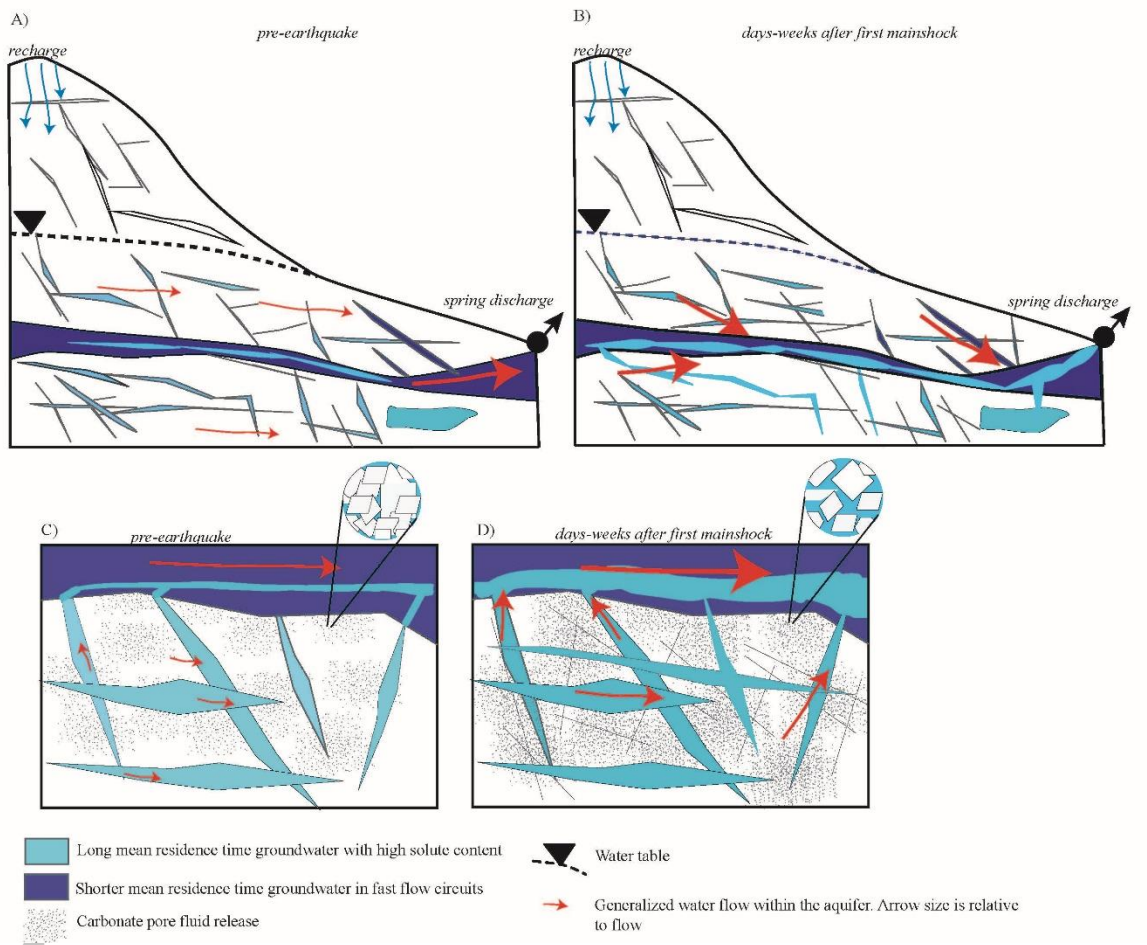

Figure 7. Conceptual model of fluid movement A) pre-earthquake and B) post-earthquake at all springs. C) pre-earthquake close-up of a section of the flow path in A, and D) post-earthquake close-up of flow path in B. Previously closed pores (C)or slow-moving water in fractures is released by shaking and pressure dilation, which releases older water that has had more time for water rock interaction with higher concentrations of trace elements than the fast-moving well-connected fractures (D). Deep-seated gas movement of CO_2 (not shown in the figure) likely also occurs along fractures at Rieti springs.